

AD-A053 249

LOWELL UNIV RESEARCH FOUNDATION MASS

F/G 4/1

THEORETICAL CALCULATIONS OF H₂O LINEWIDTHS AND PRESSURE SHIFTS:--ETC(U)

DEC 77 R W DAVIES, B A OLI

F19628-77-C-0053

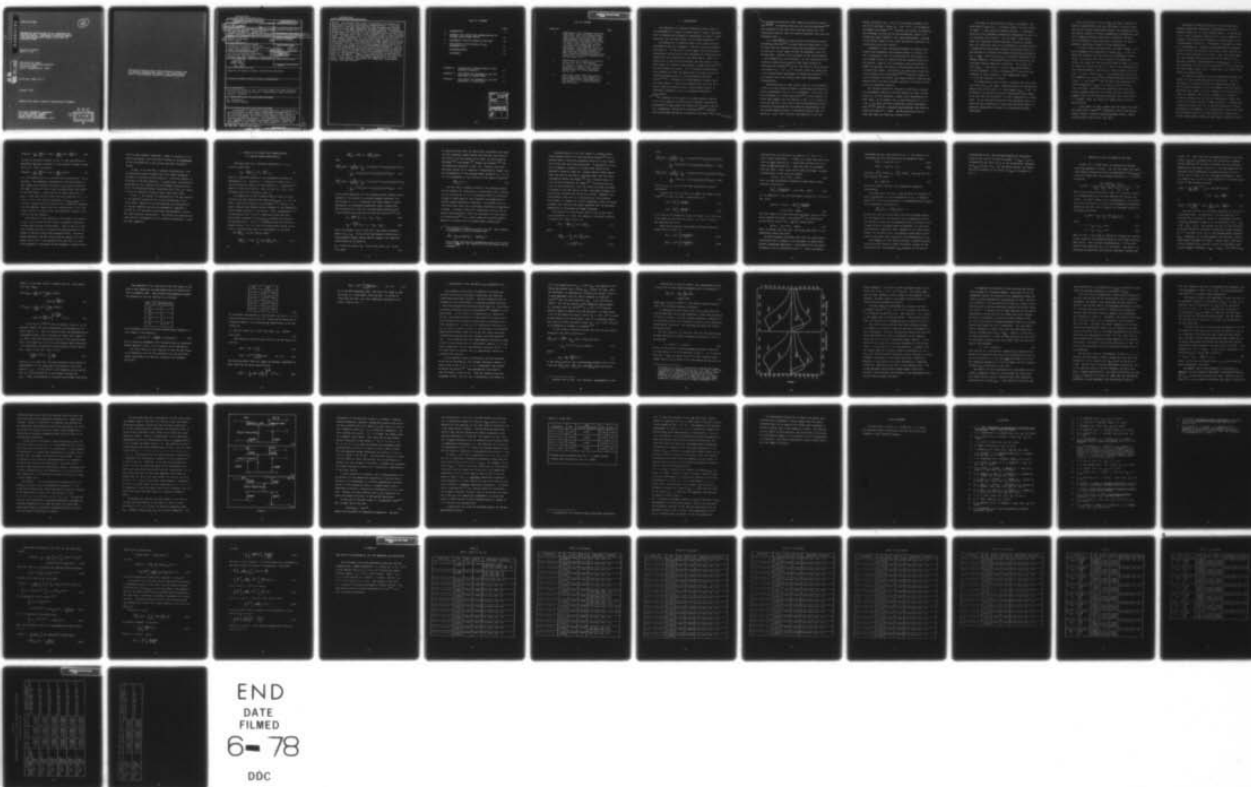
UNCLASSIFIED

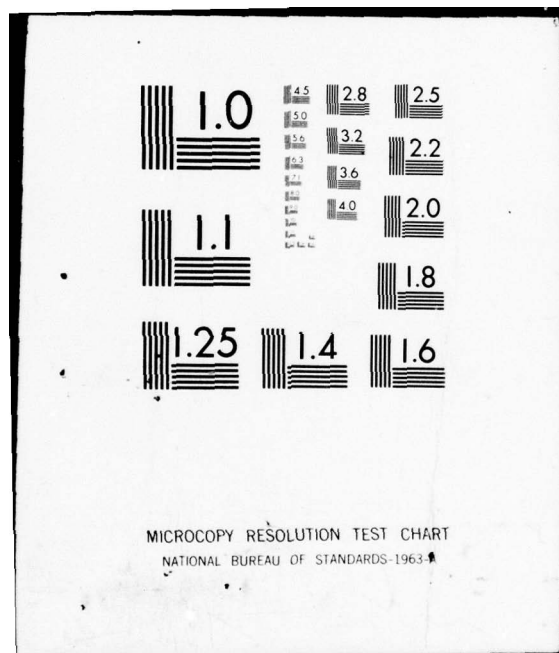
ULRF-390/CAR

AFGL-TR-78-0001

NL

1 OF 1
AD
A063249





AD A053249

AFGL-TR-78-0001

12
B.S.

THEORETICAL CALCULATIONS OF H_2O LINEWIDTHS AND
PRESSURE SHIFTS: COMPARISON OF ANDERSON THEORY
WITH QUANTUM MANY-BODY THEORY FOR N_2 AND AIR
BROADENED LINES

Richard W. Davies
Basil A. Oli

University of Lowell
Center for Atmospheric Research
450 Aiken Street
Lowell, Massachusetts 01854

Scientific Report No. 1

December 1977

Approved for public release; distribution unlimited.

AIR FORCE GEOPHYSICS LABORATORY
AIR FORCE SYSTEMS COMMAND
UNITED STATES AIR FORCE
HANSCOM AFB, MASSACHUSETTS 01731

DDC
RECEIVED
APR 27 1978
B

AD No. _____
DDC FILE COPY

Qualified requestors may obtain additional copies from the Defense Documentation Center. All others should apply to the National Technical Information Service.

UNCLASSIFIED

SECURITY CLASSIFICATION OF THIS PAGE (When Data Entered)

19 REPORT DOCUMENTATION PAGE		READ INSTRUCTIONS BEFORE COMPLETING FORM
1. REPORT NUMBER 18 AFGL-TR-78-8001	2. GOVT ACCESSION NO.	3. RECIPIENT'S CATALOG NUMBER
4. TITLE (and Subtitle) 6 THEORETICAL CALCULATIONS OF H ₂ O LINEWIDTHS AND PRESSURE SHIFTS: COMPARISON OF ANDERSON THEORY WITH QUANTUM MANY-BODY THEORY FOR N ₂ AND AIR BROADENED LINES	5. TYPE OF REPORT & PERIOD COVERED Scientific Report No. 1	6. PERFORMING ORG. REPORT NUMBER ULRF-390/CAR SCIENTIFIC-1
7. AUTHOR 10 Richard W. Davies Basil A. Oli	8. CONTRACT OR GRANT NUMBER(s) F19628-77-C-0053	9. PERFORMING ORGANIZATION NAME AND ADDRESS University of Lowell, Center for Atmospheric Research, 450 Aiken Street, Lowell, Massachusetts 01854
10. PROGRAM ELEMENT, PROJECT, TASK AREA & WORK UNIT NUMBERS 61102F 2310GLAF 17 GL	11. CONTROLLING OFFICE NAME AND ADDRESS Air Force Geophysics Laboratory Hanscom AFB, Massachusetts 01731 Contract Monitor: Francis X. Kneizys/OPI	12. REPORT DATE December 1977
13. NUMBER OF PAGES 76	14. MONITORING AGENCY NAME & ADDRESS (if different from Controlling Office) 12 73p.	15. SECURITY CLASS. (of this report)
15a. DECLASSIFICATION/DOWNGRADING SCHEDULE		
16. DISTRIBUTION STATEMENT (of this Report) Approved for public release; distribution unlimited.		
17. DISTRIBUTION STATEMENT (of the abstract entered in Block 20, if different from Report)		
18. SUPPLEMENTARY NOTES A manuscript based on this scientific report has been accepted for publication by the Journal of Quantitative Spectroscopy and Radiative Transfer.		
19. KEY WORDS (Continue on reverse side if necessary and identify by block number) H ₂ Linewidths H ₂ O Pressure Shifts		
20. ABSTRACT (Continue on reverse side if necessary and identify by block number) Comparisons of theoretical predictions for line-widths and pressure shifts of water vapor transitions broadened by N ₂ or air are presented using the Anderson-Tsao-Curnutte (ATC) theory of pressure broadening, and a more recent formalism derived using quantum many-body techniques. The theoretical predictions are also compared to available experimental results, including 110 measurements of half widths, and eight measured v ₂ -band line		

UNCLASSIFIED

SECURITY CLASSIFICATION OF THIS PAGE(When Data Entered)

shifts. The standard ATC theory for multipole interactions is generalized to yield second-order pressure shifts. It is also shown that a scaling transformation from the momentum transfer variable to the impact parameter variable converts the quantum theory to a form very similar to the ATC equations. The essential modification is to replace the ATC resonance functions $f(k)$, $F(k)$ by new functions $g(k)$, $G(k)$, which, however, have a very different shape. In particular, $g(k)$ is a Gaussian, which results from the simultaneous constraints of a Boltzmann distribution of velocities, coupled with strict momentum and energy conservation in the collision processes. The implication is that highly non-resonant collisions, i.e. collisions involving large inelasticities, are given much less weight in the quantum-derived formalism. The results are analyzed for both high and low J transitions, including the behavior of the anomalously narrow lines measured by Eng and others at high J , and the theoretical dependence of such transitions on the parameter b_{\min} used in the earlier calculations of Benedict and Kaplan. Limited comparisons are made for individual level shifts, and for the temperature dependence of the half width. Some specific suggestions for additional experimental studies are also offered.

TABLE OF CONTENTS

	Page
1. INTRODUCTION	1
2. REVIEW OF ATC THEORY WITH GENERALIZATION TO INCLUDE SECOND-ORDER SHIFTS	11
3. REDUCTION OF THE QFT THEORY TO ATC FORM	19
4. APPLICATION OF THE THEORIES TO H ₂ O BROADENED BY N ₂	27
ACKNOWLEDGEMENTS	45
REFERENCES	46
APPENDIX A SECOND-ORDER PRESSURE SHIFTS IN THE ANDERSON FORMALISM	49
APPENDIX B HALF WIDTHS FOR MEASURED N ₂ (OR AIR) BROADENED H ₂ O TRANSITIONS	55
APPENDIX C LINE SHIFTS FOR MEASURED N ₂ (OR AIR) BROADENED H ₂ O TRANSITIONS	67

ACCESSION for		
NTIS	White Section	<input checked="" type="checkbox"/>
DDC	Buff Section	<input type="checkbox"/>
UNANNOUNCED		<input type="checkbox"/>
JUSTIFICATION _____		
BY _____		
DISTRIBUTION/AVAILABILITY CODES		
Dist.	AVAIL.	and/or SPECIAL
A		

LIST OF FIGURES

Figure No.		Page
1	Comparison of ATC resonance functions $f(k)$, $F(k)$, and their Hilbert transforms $f(k)$, $F(k)$, with the QFT resonance functions $g(k)$, $G(k)$, and associated Hilbert transforms $g(k)$, $G(k)$. The plot is for the case $\alpha = (10\pi)^{1/4} = 2.36749$, which makes the theories identical for on-resonance ($k \rightarrow 0$) collisions. Note that the k -scale for the Hilbert transforms is twice the scale for the resonance functions. The resonance functions are even functions of k ; the Hilbert transforms are odd functions of k .	30
2	Theoretical half widths as a function of b_{\min} for the v_2 transitions 15, 0, 15 \rightarrow 16, 1, 16. The theoretical result $\sigma = \pi b_{\min}^2$ ($\sigma_{L,R} = 0$) is indicated by crosses. The experimental result is culled from Refs. 12, 13, 14.	35
3	Individual level shifts for three v_2 band transitions. The symbols I, F denote unperturbed level positions; the symbols I', F' denote pressure-shifted levels.	39

1. INTRODUCTION

The absorption of infrared radiation by water vapor in the atmosphere is of great interest since it plays a prominent role in determining atmospheric transmission to solar or laser radiation, and the heat balance of the lower atmosphere.⁽¹⁾

The absorption of radiation near a line center requires knowledge of the line strength S , and the collision-broadened half width γ . In the case of water vapor, very few accurate measurements of half widths were available for comparison with theoretical calculations until the early 1960's. With the improvement in grating spectrometers, and the advent of tunable lasers for infrared spectroscopy, a larger data base⁽²⁻¹⁶⁾ is now available for study. One of the more interesting recent advances has been the application of tunable lasers for accurate determinations of collision-induced pressure shifts.⁽¹²⁻¹⁴⁾ Although shift measurements for water vapor are still sparse, it may be anticipated that this will be an area of some continuing interest, particularly because it furnishes a diagnostic tool for analyzing theoretical calculations.

→ The purpose of this paper is to make specific comparisons of two theoretical methods with available experimental measurements of H_2O widths and shifts for the case of N_2 (or air) broadening. The earliest calculations⁽¹⁷⁾ of H_2O-N_2 half widths were carried out by Benedict and Kaplan (BK) using

→ over

the Anderson-Tsao-Curnutte (ATC) theory of pressure broadening. ~~(18-20)~~ Considering that only one accurate measurement ⁽²⁾ was available at the time their work was carried out, the theoretical results, with one notable exception, have stood up remarkably well.

In a comprehensive review article on microwave pressure broadening, Birnbaum ⁽²¹⁾ has made detailed comparisons of predictions from the Anderson theory with experimental results. In the case of water vapor he finds the agreement less than satisfactory. However, his indictment of the theory appears to rest primarily on the following: (a) the theoretical half widths are substantially smaller than those observed by Sanderson and Ginsburg, ⁽⁸⁾ and (b) the value of the N_2 quadrupole moment, $Q_2 = 2.46 \times 10^{-26}$ esu-cm², which was used by BK to fit the microwave measurement of Becker and Autler, ⁽²⁾ is much smaller than that obtained from other experimental determinations.

Concerning both of these points, part of the discrepancy is due to an error which BK made in correcting the Becker and Autler measurement from air to N_2 broadening. This error has been discussed in a later publication ⁽²²⁾ by the authors, in which they suggest that the results in Ref. (17) be taken as valid for dry air, while results for N_2 -broadening should be obtained by increasing the air widths by approximately 12%. Our present Anderson theory calculations indicate that one needs $Q_2 = 3.00 \times 10^{-26}$ esu-cm² (for pure N_2) to fit the

Becker and Autler line. This is in excellent agreement with the "best available" value, $Q_2 = 3.04 \times 10^{-26}$, as recommended by Stogryn and Stogryn.⁽²³⁾ Secondly, the results of Sanderson and Ginsburg, for both N_2 and self-broadening, appear to be anomalously high compared to all other measurements, although no new results appear to have been reported for precisely the transitions which they studied.

Comparison of the (corrected) Benedict and Kaplan calculations with subsequent measurements seems to indicate, for low J transitions, that the predictions for half widths (on the average) tend to be smaller than the observed values by a few percent. Some of this discrepancy could undoubtedly be removed by placing less weight on the microwave line used to calibrate the theory. Furthermore, the more recent high resolution tunable laser measurements⁽¹⁰⁻¹⁵⁾ generally appear to lead to narrower line widths than those obtained using grating spectrometers, for which somewhat uncertain slit-width corrections are frequently required.

The "notable exception" referred to previously concerns the discrepancy between the BK half widths for high J transitions ($J \geq 13$) and subsequent tunable laser measurements for such lines. As an example, the v_2 band transition 15, 0, 15 + 16, 1, 16, which has been extensively studied experimentally,⁽¹¹⁻¹⁴⁾ exhibits a measured (N_2 -broadened) half width of $0.0072 \text{ cm}^{-1}/\text{atm}$ at $T \approx 300^\circ\text{K}$. The BK calculated value is $0.032 \text{ cm}^{-1}/\text{atm}$, too large by a factor of 4.4.

The origin of the BK result is easy to elucidate. The half width is given by $\gamma = (nv/2\pi c)\sigma$, where c is the velocity of light, v = mean relative thermal velocity, n = perturber density at one atmosphere pressure and temperature T , and σ is the collision cross section. For the high J transitions, where the long-range dipole-quadrupole interaction becomes weak (the collisions are very non-resonant), the cross section is dominated by short-range repulsive interactions which are approximated by classical hard sphere scattering according to $\sigma_{HS} = \pi b_{min}^2$. Here BK take b_{min} to represent essentially the minimum "physically believable" value of the cut-off for the long-range dipole-quadrupole interaction. For H_2O-N_2 , BK choose $b_{min} = 3.2\text{\AA}$, which is close to the kinetic-theory collision diameter, 3.14\AA , as determined⁽²⁴⁾ from P-V-T measurements on H_2O-N_2 mixtures. This immediately yields $\gamma = 0.032 \text{ cm}^{-1}/\text{atm}$ for $T \approx 300^\circ\text{K}$.

The experimental results seem to indicate that the effective value of b_{min} for high J transitions must be substantially smaller than the BK value, i.e. they suggest $b_{min} \approx 1.5\text{\AA}$. The alternative (or perhaps equivalent) explanation would appear to be that the true "potential" at short separations is rather mushy. We use the word "potential" here guardedly since it's clear that the interaction at very close distances cannot be rigorously formulated in terms of an interaction between "molecules".

That the effective value of b_{\min} for high J transitions might be substantially less than the kinetic collision diameter is not totally unreasonable because the determination of the kinetic diameter is heavily weighted by contributions from low J (highly occupied) states and it therefore contains little information concerning high J collisions for which a geometric hard-sphere diameter is more appropriate.

In view of these considerations, one might attempt to improve agreement with experiment by taking $b_{\min} = 1.5\text{\AA}$ as an empirical parameter and then using it in subsequent calculations. If one does this in the context of standard ATC theory, one finds that the calculated width at high J is still too large by a factor of about 1.4, due to the contribution of the dipole-quadrupole interaction to the collision cross section. In fact, letting $b_{\min} \rightarrow 0$ and determining the ATC cut-off parameter, b_0 , by the self-contained Anderson prescription $S_2(b_0) = 1$, one finds⁽²⁵⁾ that the half width saturates (becomes independent of b_{\min}) at a value of $0.010\text{ cm}^{-1}/\text{atm}$. Since the high J transitions are associated with very non-resonant dipole-quadrupole collisions, the above difficulty suggests that the ATC resonance functions $f(k)$, $F(k)$, where $k = 2\pi cb\Delta E/v$, decay too slowly for large values of the inelasticity ΔE .

In this paper, we shall compare the ATC theory for widths and shifts with a theory⁽²⁶⁾ developed by one of the present authors (R.W.D.) based on quantum many-body theory. Henceforth we shall refer to Ref. (26) and I.

Although the theory developed in I was derived using graphical many-body techniques, the differences with the Anderson theory are of a more mundane nature. In particular, to the level of analysis carried out in I, both theories correspond to perturbation developments to second order in the intermolecular interaction. Furthermore, although the theory in I corresponds to a complete quantum-mechanical treatment, noting the fact that molecules are heavy, actual quantum corrections can be expected to be small. Also, for cases where the lowest-order vertex corrections can be ignored in the many-body treatment [corresponding to $S_2(b)_{\text{middle}} = 0$ in the ATC formalism], the basic results derived in I can be obtained much more simply using Fermi's "Golden Rule" for second-order transition probabilities.

For practical purposes, the main differences between the theory of I and the ATC approach are as follows: (a) the treatment in I rigorously conserves momentum and energy in the collision processes (in the ATC approach both the angular deflection and change in kinetic energy of the colliding molecules are ignored), and (b) the treatment in I includes a Boltzmann average over the initial translational states (ATC simply use the mean relative thermal velocity). Although the treatment of points (a), (b) in the ATC formalism is usually considered to be adequate, the justification is far from clear for collisions close to the hard sphere limit (where relatively large angular deflections may occur), and/or for colli-

sions involving large changes in internal energy (large inelasticities), where the concomitant change in kinetic energies may also be appreciable. As will be outlined briefly below, one immediate consequence of the simultaneous constraints of energy and momentum conservation, coupled with a Boltzmann distribution of velocities, is that off-resonance collisions decay as a Gaussian. This is a much more rapid decay than obtains from the ATC formalism, and in general, the shapes of the resonance functions in the two approaches are quite different.

The quantum theory developed in I is made tractable through the use of the spatial Fourier transform of the multipole interactions. Henceforth, we shall refer to the theory in I as the Quantum Fourier Transform (QFT) treatment. In this method, one writes the various multipole interactions as

$$V(\underline{R}) = \frac{1}{(2\pi)^3} \int d^3\underline{q} V(\underline{q}) e^{i\underline{q} \cdot \underline{R}}, \quad (1)$$

where $\underline{R} = \underline{R}_1 - \underline{R}_2$ is the molecular separation, with $\underline{R}_1, \underline{R}_2$ the center-of-mass coordinates. The advantage of eqn (1) for a quantum treatment is that the unperturbed wave functions governing translational motion are plane waves having the form $\psi_{\underline{k}_1}(\underline{R}_1) = e^{i\underline{k}_1 \cdot \underline{R}_1}$, $\psi_{\underline{k}_2}(\underline{R}_2) = e^{i\underline{k}_2 \cdot \underline{R}_2}$. Matrix elements of the operator $e^{i\underline{q} \cdot \underline{R}}$ are then trivial to calculate.

Subsequent reduction, using second-order perturbation theory, leads to the result that the probability per unit time of encountering a collision involving a total change in

internal energy ΔE , and with momentum transfer $\hbar q$, is proportional to

$$P(\hbar q, \Delta E) = \int d^3 \underline{k}_1 \int d^3 \underline{k}_2 \rho(\epsilon_{\underline{k}_1}) \rho(\epsilon_{\underline{k}_2}) \cdot \delta[\epsilon_{\underline{k}_1 - \underline{q}} - \epsilon_{\underline{k}_1} + \epsilon_{\underline{k}_2 + \underline{q}} - \epsilon_{\underline{k}_2} + \Delta E] . \quad (2)$$

Here $\rho(\epsilon_{\underline{k}_1})$, $\rho(\epsilon_{\underline{k}_2})$ are the Boltzmann translational functions for molecules 1, 2, with $\epsilon_{\underline{k}_1} = \hbar^2 \underline{k}_1^2 / 2m_1 = \underline{p}_1^2 / 2m_1$ and similarly for $\epsilon_{\underline{k}_2}$. It should be noted that the quantity $\hbar q$, where \underline{q} is the Fourier transform variable introduced in eqn (1), is precisely the classical momentum transfer in the collision process. The double integration in eqn (2) may be carried out directly using the method outlined in Appendix B of Ref. (1); however, it is much simpler to introduce the transformation to center-of-mass and relative coordinates via

$$\underline{k}_1 = \underline{k} + m_1 / (m_1 + m_2) \underline{K} ,$$

$$\underline{k}_2 = - \underline{k} + m_2 / (m_1 + m_2) \underline{K} .$$

The Jacobian of the above transformation is unity, and the transformation factorizes the double integral to give

$$P(\hbar q, \Delta E) = \frac{1}{Z} \int d^3 \underline{K} e^{-\beta \frac{\hbar^2 K^2}{2M}} \int d^3 \underline{k} e^{-\beta \frac{\hbar^2 k^2}{2m}} \delta[-\frac{\hbar^2 \underline{k} \cdot \underline{q}}{m} + \frac{\hbar^2 q^2}{2m} + \Delta E] , \quad (3a)$$

where $Z = [2\pi\sqrt{m_1 m_2} / (\beta \hbar^2)]^3$, $\beta = 1/k_B T$, $M = (m_1 + m_2)$, and $m = m_1 m_2 / M$ is the reduced mass. Evaluation is straightforward and gives

$$P(\hbar q, \Delta E) = \frac{1}{\sqrt{2\pi}} \left(\frac{\beta m}{\hbar^2 q^2} \right)^{1/2} \exp \left[- \frac{\beta m}{2\hbar^2 q^2} \left(\Delta E + \frac{\hbar^2 q^2}{2m} \right)^2 \right] . \quad (3b)$$

As will be discussed further in Sec. 3, the term $\hbar^2 q^2/2m$ is generally negligible compared to the (quantum allowed) inelasticity ΔE . Then one obtains

$$P(\hbar q, \Delta E) = \frac{1}{\sqrt{2\pi}} \left(\frac{\beta m}{\hbar^2 q^2} \right)^{1/2} \exp \left[- \frac{\beta m}{2\hbar^2 q^2} (\Delta E)^2 \right] , \quad (4)$$

i.e. the probability of a collision with inelasticity = ΔE is Gaussian. The immediate consequence of the above result is that highly non-resonant collisions, e.g. H_2O-N_2 collisions for high J levels of water vapor, are given much less weight in the QFT theory. In particular, we shall show, down to $b_{\min} = 1.5\text{\AA}$, that the QFT theory for the transition 15, 0, 15 \rightarrow 16, 1, 16 is very nearly equivalent to $\sigma_{\text{dipole-quad.}} = 0$. For low J transitions, our results lead to essential agreement with the Anderson theory, and this corroboration is not completely trivial in view of the very different resonance functions in the two theories.

The outline of the remainder of the paper is as follows. In Sec. 2, we review the ATC theory of pressure broadening arising from multipole interactions. This is done to establish notation and also to present the generalization of the theory to include second-order pressure shifts. The above generalization of the ATC theory does not appear to be well-known, and in Sec. 2 and Appendix A we show that it essentially amounts to replacing the ATC resonance functions $f(k)$,

$F(k)$ by their Hilbert transforms. Then, in contrast to the width calculation, the line shift is given by the difference of the contributions in the initial and final radiative states.

In Sec. 3, we show that a scaling transformation, from the momentum transfer variable $\hbar q$ to the impact parameter variable b , converts the QFT theory to a form very similar in structure to the ATC equations. In particular, the essential modification is to replace the ATC resonance functions $f(k)$, $F(k)$, and associated Hilbert transforms $\check{f}(k)$, $\check{F}(k)$, by a modified set of resonance functions $g(k)$, $G(k)$, $\tilde{g}(k)$, $\tilde{G}(k)$.

In Sec. 4, we discuss the application of the two theories to the specific problem of N_2 (or air) broadening of H_2O transitions. Details of the calculations are described and the actual numerical results are presented in Appendix B (widths for 110 measured transitions) and Appendix C (shifts for eight measured transitions). The results are analyzed and some specific recommendations for further experimental studies are also suggested.

2. REVIEW OF ATC THEORY WITH GENERALIZATION TO INCLUDE SECOND-ORDER SHIFTS

The half width for a radiative transition $i \rightarrow f$, is given by ($\text{cm}^{-1}/\text{atm}$)

$$\gamma_{if} = \left(\frac{nv}{2\pi c}\right) \sum_{J_2} \rho(J_2) \sigma_{if, J_2}^{(R)}, \quad (5)$$

where n = perturber density at one atmosphere pressure and temperature T ($n = n_0 273/T$), c = velocity of light, and v is the mean relative thermal velocity given by $v = [8k_B T/(\pi m)]^{1/2}$, where m is the reduced mass. Also, in eqn (5), $\rho(J_2)$ is the Boltzmann factor for perturber state J_2 .

For simplicity in the treatment which follows, we shall consider the case where the ATC term $S_2(b)_{\text{middle}} = 0$. For the case of particular interest in this paper, i.e. $\text{H}_2\text{O}-\text{N}_2$, this results because the diagonal matrix elements of the (permanent) dipole moment operator of H_2O vanish. Also, independently of the particular case, it may be rigorously shown that the second-order treatment of $S_2(b)_{\text{middle}}$ contributes nothing to the pressure shift. This is in agreement with the conclusion reached in Ref. (1), i.e. that the lowest-order vertex corrections in the QFT theory make no contribution to the shift.

For $\sigma_{if, J_2}^{(R)}$, the ATC theory yields

$$\sigma_{if, J_2}^{(R)} = \pi [b_0^2 + \int_{b_0}^{\infty} 2b db s_{if, J_2}^{(R)}(b)], \quad (6a)$$

or

$$\sigma_{if,J_2}^{(R)} = \pi b_0^2 [1 + S_{if,J_2}^{(R)}(b_0)] , \quad (6b)$$

with

$$S_{if,J_2}^{(R)}(b_0) = \left(\frac{c_n''}{\hbar^2 v^2 b_0^n} \right) \left\{ \sum_{J_2' i'} |\langle i || O_1 || i' \rangle|^2 |\langle J_2 || O_2 || J_2' \rangle|^2 f(k_i) \right. \\ \left. + \sum_{J_2' f'} |\langle f || O_1 || f' \rangle|^2 |\langle J_2 || O_2 || J_2' \rangle|^2 f(k_f) \right\}, \quad (7a)$$

$$S_{if,J_2}^{(R)}(b_0) = \left(\frac{c_n''}{\hbar^2 v^2 b_0^n} \right) \left\{ \sum_{J_2' i'} |\langle i || O_1 || i' \rangle|^2 |\langle J_2 || O_2 || J_2' \rangle|^2 F(k_{i0}) \right. \\ \left. + \sum_{J_2' f'} |\langle f || O_1 || f' \rangle|^2 |\langle J_2 || O_2 || J_2' \rangle|^2 F(k_{f0}) \right\}. \quad (7b)$$

In the above equations, we have denoted various reduced matrix elements of the dipole or quadrupole moment operators, and the indices $n = 4, 6, 8$ represent the dipole-dipole, dipole-quadrupole, and quadrupole-quadrupole cases, respectively. The functions $f(k)$, $F(k)$ are the well-known resonance functions discussed and tabulated by Tsao and Curnutte,⁽²⁰⁾ and

$$k_i = \frac{2\pi c b}{v} (E_i - E_{i'} + E_{J_2} - E_{J_2'}) , \quad (8a)$$

$$k_{i0} = \frac{2\pi c b_0}{v} (E_i - E_{i'} + E_{J_2} - E_{J_2'}) , \quad (8b)$$

where the energies are in units cm^{-1} , and similar formulas apply to k_f , k_{f0} . If we use the Tsao-Curnutte definition of the quadrupole moment reduced matrix element, the numerical coefficients c_n'' are given by

$$c_4'' = (4/9) \text{ (d-d case)}, c_6'' = (4/45) \text{ (d-q case)}, c_8'' = (1/25) \text{ (q-q case)}. \quad (9)$$

It should be noted that the definition of Benedict and Kaplan for the quadrupole moment agrees with the Tsao and Curnutte definition, but this definition is twice the value used by Birnbaum,⁽²¹⁾ Buckingham,⁽²⁷⁾ Stogryn and Stogryn,⁽²³⁾ and the definition employed[†] in Ref. (I). Finally, the above equations assume use of Anderson's "approximation number two" for determination of the minimum impact parameter b_0 , i.e. b_0 is to be determined as the solution of the implicit equation

$$s_{if,J_2}^{(R)}(b_0) = 1. \quad (10)$$

We turn next to pressure shifts in the Anderson theory. In the original ATC formulation, a first-order shift contribution is calculated, but the second-order shift is eliminated through an approximation which neglects non-commutivity of certain quantum mechanical operators. As pointed out in I, the first-order shift due to multipole interactions rigorously vanishes. Although "effective" interactions such as the induction and dispersion forces can contribute in first order, it is well-known⁽¹⁸⁾ that these forces are actually approximations to second-order (or higher-order) interactions.

† The statement following eqn (5.17) in Ref. (26) contains a typographical error and should read

$$|Q_b|^{\leftrightarrow} = \sum_{\beta} e_{b\beta} [f_{\beta}(b)_{z'z'}^2 - f_{\beta}(b)_{x'x'}^2].$$

For a charge distribution possessing an axis (z') of sufficient symmetry, this agrees with the definition used by Birnbaum.⁽²¹⁾

A generalization of the ATC theory to include second-order pressure shifts has been derived by Herman⁽²⁸⁾ for the special case of induction-dispersion forces (for the interaction of HCL with inert gas molecules). In Appendix A, we derive the general formulas for second-order shifts using Anderson's original formalism. Rather similar formal expressions can also be obtained as limiting cases from the theory developed by Murphy and Boggs,⁽²⁹⁾ and a related theory recently given by Mehrotra and Boggs.⁽³⁰⁾ We should also mention, in this connection, that the theory of Murphy and Boggs is similar to the QFT theory in that a Boltzmann average over the initial translational states is included. However, computationally, when used in conjunction with the classical path method, it appears to be more cumbersome, since the double integral over velocity and impact parameter must be performed numerically in the Murphy and Boggs formalism.

The results for second-order shifts from the ATC theory can be expressed in a form very similar to the width formulas. The shift ($\text{cm}^{-1}/\text{atm}$) is given by

$$\Delta\gamma_{if} = \left(\frac{nv}{2\pi c}\right) \sum_{J_2} \rho(J_2) \sigma_{if,J_2}^{(I)}, \quad (11)$$

where

$$\sigma_{if,J_2}^{(I)} = \pi \int_{b_0}^{\infty} 2b db s_{if,J_2}^{(I)}(b), \quad (12a)$$

$$= \pi b_0^2 S_{if}^{(I)}(b_0), \quad (12b)$$

with

$$s_{if,J_2}^{(I)}(b) = \left(\frac{c_n''}{\hbar^2 v^2 b^n}\right) \left\{ \sum_{J_2' i'} | \langle i | | 0_1 | | i' \rangle |^2 | \langle J_2 | | 0_2 | | J_2' \rangle |^2 \tilde{f}(k_i) \right. \\ \left. - \sum_{J_2' f'} | \langle f | | 0_1 | | f' \rangle |^2 | \langle J_2 | | 0_2 | | J_2' \rangle |^2 \tilde{f}(k_f) \right\}, \quad (13a)$$

$$s_{if,J_2}^{(I)}(b_0) = \left(\frac{c_n''}{\hbar^2 v^2 b_0^n}\right) \left\{ \sum_{J_2' i'} | \langle i | | 0_1 | | i' \rangle |^2 | \langle J_2 | | 0_2 | | J_2' \rangle |^2 \tilde{F}(k_{i0}) \right. \\ \left. - \sum_{J_2' f'} | \langle f | | 0_1 | | f' \rangle |^2 | \langle J_2 | | 0_2 | | J_2' \rangle |^2 \tilde{F}(k_{f0}) \right\}, \quad (13b)$$

and k_i, k_{i0}, k_f, k_{f0} have the same definitions as given previously.

In eqn (13), $\tilde{f}(k)$ and $\tilde{F}(k)$ are simply the Hilbert transforms⁽³¹⁾ of $f(k)$ and $F(k)$, respectively, i.e.

$$\tilde{f}(k) = \frac{\text{Pr}}{\pi} \int_{-\infty}^{\infty} \frac{f(k') dk'}{k' - k}, \quad (14a)$$

$$\tilde{F}(k) = \frac{\text{Pr}}{\pi} \int_{-\infty}^{\infty} \frac{F(k') dk'}{k' - k}. \quad (14b)$$

It is also to be understood in eqn (14) that $f(k'), F(k')$ are to be taken as even functions of k' , i.e. $f(k') = f(|k'|)$, and similarly for $F(k')$.

Some useful formulas connecting the various functions should also be noted, viz.

$$F(k) = 2k^{n-2} \int_k^{\infty} \frac{k' dk' f(k')}{k'^n}, \quad (15a)$$

$$\tilde{F}(k) = 2k^{n-2} \int_k^{\infty} \frac{k' dk' \tilde{f}(k')}{k'^n}. \quad (15b)$$

Equations (15) are valid for the case $k > 0$. For $k < 0$, $F(k) = F(|k|)$ while $\tilde{F}(k) = -F(|k|)$, i.e. $f(k)$, $F(k)$ are to be taken as even functions of k , while $\tilde{f}(k)$ and $\tilde{F}(k)$ are to be taken as odd functions of k . That eqn (15b) is consistent with eqn (14a), (14b), (15a) can be seen as follows. We take the derivative of eqn (15a) and obtain

$$kF'(k) = (n-2)F(k) - 2f(k). \quad (16)$$

Next, we take the Hilbert transform of both sides of this equation, which gives

$$\frac{\text{Pr}}{\pi} \int_{-\infty}^{\infty} \frac{k'F'(k')dk'}{k'-k} = (n-2)\tilde{F}(k) - 2\tilde{f}(k). \quad (17)$$

In the numerator of the left-hand-side, we write $k' = (k'-k) + k$. This gives

$$\begin{aligned} \frac{1}{\pi} [F(\infty) - F(-\infty)] + k \frac{\text{Pr}}{\pi} \int_{-\infty}^{\infty} \frac{F'(k')dk'}{k'-k} \\ = (n-2)\tilde{F}(k) - 2\tilde{f}(k). \end{aligned} \quad (18)$$

The first term on the left-hand-side vanishes, and, by a well-known theorem for Hilbert transforms,⁽³¹⁾ the second term equals $k\tilde{F}'(k)$, where $\tilde{F}'(k) \equiv \frac{d}{dk} \tilde{F}(k)$, which gives

$$k\tilde{F}'(k) = (n-2)\tilde{F}(k) - 2\tilde{f}(k). \quad (19)$$

Then, by analogy with eqn (16), and noting that $\tilde{F}(\infty) = 0$, we immediately obtain eqn (15b).

The ATC resonance functions $f(k)$, $F(k)$ are sufficiently complicated that it appears to be necessary to obtain their Hilbert transforms numerically. Such results for the dipole-quadrupole case are presented in Sec. 4. Since the Hilbert

transforms are odd, they vanish at $k = 0$. For large k , one can easily see that they must have the asymptotic form

$$\tilde{f}(k) = -\beta_s/k \quad (k \rightarrow \infty), \quad (20a)$$

$$\tilde{F}(k) = -\beta_\ell/k \quad (k \rightarrow \infty), \quad (20b)$$

where $\beta_s = \frac{1}{\pi} \int_{-\infty}^{\infty} f(k)dk$, $\beta_\ell = \frac{1}{\pi} \int_{-\infty}^{\infty} F(k)dk$. From eqn (19) one then obtains the result

$$\beta_\ell = \left(\frac{2}{n-1}\right) \beta_s, \quad (21)$$

which is a useful relation for checking the numerical calculations.

One final point to note is that we have not included the shift contribution in the determination of b_0 . In Herman's paper,⁽²⁸⁾ a cut-off prescription is recommended which appears to be essentially equivalent to

$$s_{if,J_2}^{(R)}(b_0) + |s_{if,J_2}^{(I)}(b_0)| = 1.$$

We will not use this prescription for the following reasons:

- (a) the theoretical justification is not completely obvious,
- (b) we want to keep the correspondence with the earlier calculations of BK as straightforward as possible,
- (c) the shift contribution is generally small compared to the width contribution, so, for most cases, one expects rather small corrections if the shift were included in the determination of b_0 .

The formulas in this Section provide a complete description of the ATC theory of widths and shifts, except for the introduction of the parameter b_{\min} employed in the earlier

calculations of BK. This minimum "physically believable" value of the cut-off is used as follows: if $b_{\min} < b_0$ [as determined by eqn (10)] use b_0 in the calculation, otherwise use b_{\min} in place of b_0 . For the H_2O-N_2 system, the dependence of the results on the choice of b_{\min} is discussed in Sec. 4.

3. REDUCTION OF THE QFT THEORY TO ATC FORM

In Ref. (I), the QFT theory of second-order pressure shifts was analyzed in detail. For the case where the lowest-order vertex corrections vanish [corresponding to $S_2(b)_{\text{middle}} = 0$ in the ATC formalism], the lineshape function ($\mu' + \mu$) can be written as

$$f_{\mu',\mu}(\hbar\omega) = \int \frac{d^3\mathbf{k} \rho(\epsilon_{\mathbf{k}}^a)(\Gamma_{\mu\mathbf{k}} + \Gamma_{\mu'\mathbf{k}})}{(E_{\mu\mathbf{k}}^a - E_{\mu'\mathbf{k}}^a - \hbar\omega)^2 + (\Gamma_{\mu\mathbf{k}} + \Gamma_{\mu'\mathbf{k}})^2} . \quad (22)$$

Here we are using the notation of Ref. (I). We will indicate the correspondence with the more familiar ATC notation presently. In order to make such a correspondence, it is necessary (also convenient) to ignore the inhomogeneous broadening implied by eqn (22), and to replace the lineshape function by the simple Lorentzian

$$f_{\mu',\mu}(\hbar\omega) = \frac{\Gamma}{(\epsilon_{\mu}^a - \epsilon_{\mu'}^a - \Delta - \hbar\omega)^2 + \Gamma^2} , \quad (23)$$

where

$$\Gamma = \langle \Gamma_{\mu\mathbf{k}} + \Gamma_{\mu'\mathbf{k}} \rangle_{\text{ave}} , \quad (24)$$

$$\Delta = \langle \Delta_{\mu\mathbf{k}} - \Delta_{\mu'\mathbf{k}} \rangle_{\text{ave}} . \quad (25)$$

Here $\langle 0 \rangle_{\text{ave}} = \int d^3\mathbf{k} \rho(\epsilon_{\mathbf{k}}^a) 0_{\mathbf{k}}$ implies an average over translational states of the absorbing molecule, with $\rho(\epsilon_{\mathbf{k}}^a)$ the Boltzmann factor. With the above approximations, Γ is the half width of the Lorentzian and $-\Delta$ is the shift. The object Δ is precisely the quantity calculated for multipole interactions

in Ref. (I). Since the real and imaginary parts of the self-energy ($\Delta_{\mu\mathbf{k}}$ and $\Gamma_{\mu\mathbf{k}}$ respectively) are connected by Kramers-Kronig relations, it is easy to see that the only essential modification necessary to obtain Γ is the replacement of the principal value denominators in equations such as (5.10), (5.19), (B.1) of Ref. (I) by $\pi \delta(\text{energy denominator})$. Thus for example, eqn (5.19) of I gets replaced in the width calculation by the resonance function

$$\Gamma_q(\Delta E_\mu) = \frac{1}{\sqrt{2\pi}} \left(\frac{\beta m}{\hbar^2 q^2} \right)^{1/2} \int_{-\infty}^{\infty} dE' \exp[-\beta m E'^2 / 2\hbar^2 q^2] \cdot \pi \delta(E' - \Delta E_\mu - \frac{\hbar^2 q^2}{2m}), \quad (26)$$

or

$$\Gamma_q(\Delta E_\mu) = \sqrt{\frac{\pi}{2}} \left(\frac{\beta m}{\hbar^2 q^2} \right)^{1/2} \exp\left[-\frac{\beta m}{2\hbar^2 q^2} \left(\Delta E_\mu + \frac{\hbar^2 q^2}{2m}\right)^2\right]. \quad (27)$$

The above results is essentially identical to eqn (3b) of the present paper. As mentioned in the Introduction, the term $\hbar^2 q^2 / 2m$, involving the square of the momentum transfer, is usually negligible compared to the inelasticity $\Delta E_\mu = (\epsilon_{\mu_1}^a - \epsilon_{\mu}^a) + (\epsilon_{\gamma_1}^b - \epsilon_{\gamma_2}^b)$. The argument for this is the following. In the ATC theory the multipole interactions become divergent as $b \rightarrow 0$ and must be cut off at some minimum impact parameter b_{\min} . Similarly, in the QFT approach, the multipole interactions become divergent at large q . Since q and b form essentially a Fourier pair, one must cut-off the multipole interactions roughly according to $q_{\max} \approx 1/b_{\min}$. Thus $(\hbar^2 q^2 / 2m)_{\max}$

$\approx (\hbar^2/2mb_{\min}^2)$. Taking $b_{\min} \approx 3\text{\AA}$, $m = 1.83 \times 10^{-23}$ grams as the reduced mass of $\text{H}_2\text{O}-\text{N}_2$, and converting the energy to cm^{-1} , yields $(\hbar^2q^2/2m)_{\max} \approx .2 \text{ cm}^{-1}$. This value is totally negligible compared to typical (quantum allowed) inelasticities, ΔE_μ , for $\text{H}_2\text{O}-\text{N}_2$ collisions. It might be noted, if the term $(\hbar^2q^2/2m)$ is retained in eqn (27), that the resulting theory for widths is formally convergent at large q (the calculation of shifts still leads to a high q divergence). However, this convergence is spurious since it occurs at values of q where the multipole interaction is totally unphysical.

From the above argument, we henceforth replace eqn (27) by the Gaussian formula

$$\Gamma_q(\Delta E_\mu) = \sqrt{\frac{\pi}{2}} \left(\frac{\beta m}{\hbar^2 q^2} \right)^{1/2} \exp\left[-\frac{\beta m}{2\hbar^2 q^2} (\Delta E_\mu)^2\right]. \quad (28)$$

Similarly, if we ignore $(\hbar^2q^2/2m)$ in comparison to ΔE_μ in eqn (5.22) of I, then eqn (5.20), (5.21) of I lead to the following resonance function for the calculation of shifts:

$$\gamma_q(\Delta E_\mu) = \left(\frac{2\beta m}{\hbar^2 q^2} \right)^{1/2} e^{-\frac{\beta m (\Delta E_\mu)^2}{2\hbar^2 q^2}} \int_0^{\frac{\beta m (\Delta E_\mu)^2}{2\hbar^2 q^2}} \left(\frac{\beta m}{2\hbar^2 q^2} \right)^{1/2} \Delta E_\mu e^{t^2} dt. \quad (29)$$

The functions $\Gamma_q(\Delta E_\mu)$ and $\gamma_q(\Delta E_\mu)$ are simply Hilbert pairs, in particular[†]

$$\gamma_q(\Delta E_\mu) = -\frac{\text{Pr}}{\pi} \int_{-\infty}^{\infty} \frac{\Gamma_q(E)dE}{E-\Delta E_\mu}.$$

[†] A simple derivation of the Hilbert transform of a Gaussian may be found in Ref. (32); see also Ref. (33).

Next one has to integrate the contribution of these functions over q . In view of eqn (5.11) of I, the shift calculation involves

$$L^{(n)}(\Delta E_\mu) = \frac{1}{(2\pi)^3} \int d^3q q^n g(q)^2 \gamma_q(\Delta E_\mu) , \quad (31a)$$

$$= 8 \int_0^\infty dq q^{n-2} e^{-2qr_c} \gamma_q(\Delta E_\mu) . \quad (31b)$$

Similarly, for the linewidth one needs

$$M^{(n)}(\Delta E_\mu) = \frac{1}{(2\pi)^3} \int d^3q q^n g(q)^2 \Gamma_q(\Delta E_\mu) , \quad (32a)$$

$$= 8 \int_0^\infty dq q^{n-2} e^{-2qr_c} \Gamma_q(\Delta E_\mu) . \quad (32b)$$

The meaning of the index n is the same as in Sec. 2, i.e. $n = 4, 6, 8$ for the dipole-dipole, dipole-quad., and quad.-quad. cases respectively.

In eqn (31b), (32b) we have also retained the phenomenological convergence factor e^{-qr_c} , which was introduced in I, where $r_c \approx b_{\min}$. We will now eliminate this parameter in favor of a cut-off procedure more closely related to Anderson's method. To do this, we introduce the scaling transformation

$$q = \alpha/b , \quad (33)$$

where, at this point, α is an arbitrary (dimensionless) constant, and the length b becomes the new variable of integration. It is also useful to eliminate β in the previous equations by using

$$\beta = 1/k_B T = 8/(\pi m v^2) , \quad (34)$$

where v is the mean relative thermal velocity. This gives,
with $\Delta E_\mu = \hbar \Delta \omega_\mu$,

$$M^{(n)}(\Delta \omega_\mu) = \left(\frac{16}{\hbar v}\right) \alpha^{n-2} \int_0^\infty \frac{b db}{b^n} e^{-2\alpha r_c/b} \cdot \exp\left[-\frac{4}{\pi} \left(\frac{b \Delta \omega_\mu}{\alpha v}\right)^2\right], \quad (35)$$

$$L^{(n)}(\Delta \omega_\mu) = \left(\frac{32}{\sqrt{\pi} \hbar v}\right) \alpha^{n-2} \int_0^\infty \frac{b db}{b^n} e^{-2\alpha r_c/b} \cdot \exp\left[-\frac{4}{\pi} \left(\frac{b \Delta \omega_\mu}{\alpha v}\right)^2\right] \int_0^{\sqrt{\frac{4}{\pi}} \left(\frac{b \Delta \omega_\mu}{\alpha v}\right)} e^{t^2} dt. \quad (36)$$

If the factor $e^{-2\alpha r_c/b}$ were not present, then, as in the Anderson theory, the above expressions are divergent at the lower limit $b \rightarrow 0$. Here we choose to drop the phenomenological convergence factor, and to replace the lower limit simply by b_0 , where, with some appropriate choice of the scaling parameter α , we regard b_0 as an effective minimum impact parameter, to be determined by Anderson's self-contained cut-off procedure. Thus, in eqn (35), (36), we let

$$\int_0^\infty \frac{b db}{b^n} e^{-2\alpha r_c/b} \rightarrow \int_{b_0}^\infty \frac{b db}{b^n}. \quad (37)$$

Finally, it is clear that the above procedure only defines an approximation to the long-range contribution to the cross section, $\sigma_{L.R.}$. In the spirit of the Anderson cut-off method, this is to be augmented by a short-range contribution, $\sigma_{S.R.} = \pi b_0^2$, corresponding to classical hard sphere scattering.

The remainder of the reduction of the QFT theory to ATC form is now completely straightforward and the details will not be presented here. Some helpful correspondence between the notation in the two theories is as follows:

Ref. (I) \rightarrow ATC Notation		
$j\mu$	\rightarrow	f
$j\mu'$	\rightarrow	i
$j\gamma_2$	\rightarrow	J_2
$j\gamma_1$	\rightarrow	J'_2
$j\mu_1$	\rightarrow	$i' \text{ or } f'$

The following relation involving reduced matrix elements is also useful in the reduction:

$$|\langle J || 0 || J' \rangle|^2 = \left(\frac{2J'+1}{2J+1} \right) |\langle J' || 0 || J \rangle|^2, \quad (38)$$

and it should be remembered that the definition of quadrupole moment employed in Ref. (I) is one-half the BK definition.

The final result of this analysis is that the QFT theory can be generated from the ATC equations with the following simple replacements of numerical constants and resonance functions:

ATC	→	QFT
$c_n'' f(k)$	→	$c_n' \frac{8}{\pi} \alpha^{n-2} g(k)$
$c_n'' F(k)$	→	$c_n' \frac{8}{\pi} \alpha^{n-2} G(k)$
$c_n'' \tilde{f}(k)$	→	$c_n' \frac{8}{\pi} \alpha^{n-2} \tilde{g}(k)$
$c_n'' \tilde{F}(k)$	→	$c_n' \frac{8}{\pi} \alpha^{n-2} \tilde{G}(k)$

(39)

In the above correspondence, the constants c_n'' , for $n = 4, 6, 8$ were previously given in eqn (9). Using the BK definition of quadrupole moment, the corresponding coefficients in the QFT theory are

$$c_4' = \frac{2}{27} \text{ (d-d case)}, c_6' = 1/900 \text{ (d-q case)}, c_8' = 1/63000$$

(q-q case).

(40)

The resonance functions $g(k)$, $G(k)$ in the QFT theory are given by

$$g(k) = \exp \left\{ -\frac{4}{\pi} \frac{k^2}{\alpha^2} \right\}, \quad (41)$$

$$G(k) = 2k^{n-2} \int_0^\infty \frac{k' dk'}{k (k')^n} g(k') \quad (k > 0). \quad (42)$$

The functions $\tilde{g}(k)$, $\tilde{G}(k)$ are simply the Hilbert transforms of $g(k)$, $G(k)$ and are given explicitly by

$$\tilde{g}(k) = -\frac{2}{\sqrt{\pi}} \exp \left[-\frac{4}{\pi} \frac{k^2}{\alpha^2} \right] \int_0^{\frac{2}{\sqrt{\pi}} \frac{k}{\alpha}} e^{t^2} dt, \quad (43)$$

$$\tilde{G}(k) = 2k^{n-2} \int_0^\infty \frac{k' dk'}{k (k')^n} \tilde{g}(k') \quad (k > 0) . \quad (44)$$

As in the ATC formalism, $g(k)$, $G(k)$ are to be taken as even functions of k , while $\tilde{g}(k)$, $\tilde{G}(k)$ are odd. It should be noted that eqn (42), (44) are completely analogous to eqn (15a), (15b) of Sec. 2.

4. APPLICATION OF THE THEORIES TO H_2O BROADENED BY N_2

The original calculations of Benedict and Kaplan were carried out for pure rotational transitions and ignoring vibrational-rotational coupling. We have attempted some refinement of the calculations by utilizing programs developed at Air Force Geophysics Laboratory which treat the vibrational-rotational coupling in H_2O via the Watson⁽³⁴⁾ asymmetric rotor Hamiltonian. In the case of the ground and ν_2 vibrational states, the present calculations are based on the best available constants for the Watson Hamiltonian as determined by a least-squares fit. In the case of transitions involving the ν_1 , ν_3 , and $2\nu_2$ states, because of the existence of accidental degeneracies between these states, we have simply performed calculations using ground-state energy levels and eigenvectors. It is doubtful that this approximation introduces large errors in the calculations of half-widths, however, it is certainly inadequate for the calculation of pressure shifts. On the other hand, at present only ν_2 experimental shifts are available for analysis.

In our Anderson theory calculations, we have proceeded as BK did by choosing Q_2 , the nitrogen quadrupole moment, to force a fit to the 5, 2, 3 \rightarrow 6, 1, 6 microwave line studied by Becker and Autler.⁽²⁾ The experimental half-width is $.087 \text{ cm}^{-1}/\text{atm}$ at 318°K in air. From the tunable laser measurements in Ref. (14) for low J transitions, one infers an

air to N_2 correction of $\gamma_{N_2} = 1.1045 \gamma_{\text{air}}$, and applied to the Becker and Autler result yields $\gamma_{N_2} = 0.0961 \text{ cm}^{-1}/\text{atm}$. When the difference in temperatures is taken into account, this is in good agreement with the result obtained by Liebe and Dillon⁽³⁾ for the same transition ($\gamma_{N_2} = 0.104 \text{ cm}^{-1}/\text{atm}$ at 300°K). For the H_2O (ground state) permanent dipole moment d_1 , we have taken the value⁽³⁵⁾ $d_1 = 1.85 \times 10^{-18} \text{ esu-cm}$, which is about 1% smaller than the BK choice. We then obtain a fit to the Becker and Autler line if $Q_2 = 3.00 \times 10^{-26} \text{ esu-cm}^2$. As mentioned in the Introduction, this is in excellent agreement with the "best available" value, $Q_2 = 3.04 \times 10^{-26} \text{ esu-cm}^2$, as recommended by Stogryn and Stogryn.⁽²³⁾

In the notation introduced by BK, eqn (7a) for the dipole-quadrupole case may be written as

$$s_{if,J_2}^{(R)}(b) = \left(\frac{A_{DQ}}{b}\right)^6 \left\{ \sum_{i,J_2'} D(i,i') Q(J_2,J_2') f(k_i) + \sum_{f,J_2'} D(f,f') Q(J_2,J_2') f(k_f) \right\}, \quad (45)$$

where[†]

$$A_{DQ} = \left[\frac{4}{45} \left(\frac{d_1 Q_2}{\hbar \nu} \right)^2 \right]^{1/6}. \quad (46)$$

In the above notation, the corresponding formulas (7b), (13a), (13b) for $s_{if,J_2}^{(R)}(b_0)$, $s_{if,J_2}^{(I)}(b)$, and $s_{if,J_2}^{(I)}(b_0)$ are obvious.

† Equation (4a) in Ref. (17) contains a typographical error.

Turning now to the QFT theory, the correspondence given in eqn (39) for the dipole-quadrupole case is equivalent to

$$\begin{aligned} A_{DQ}^6 f(k) &\rightarrow A_{DQ}^6 \left(\frac{\alpha^4}{10\pi} \right) g(k) \\ &= (A'_{DQ})^6 g(k) , \end{aligned} \quad (47)$$

where $A'_{DQ} = A_{DQ} [\alpha^4/(10\pi)]^{1/6}$, and obvious similar replacements for the other resonance functions.

In applying the QFT theory, one is now confronted with the problem that the scaling parameter α , which was introduced in order to obtain a cut-off procedure similar to Anderson's, is not given apriori, and therefore α ends up as an additional undetermined[†] quantity. Two reasonable methods for fixing α are given below.

We note from eqn (41) and (47) that the two theories may be made identical for purely resonant collision ($k \propto \Delta E \rightarrow 0$) by choosing

$$\alpha = (10\pi)^{1/4} = 2.36749 . \quad (48)$$

A plot of the various dipole-quadrupole resonance functions for this choice of α is illustrated in Fig. 1. It is obvious from Fig. 1 that the above choice of α will require a much larger value of Q_2 in order to fit the Becker and Autler line.

[†] From eqn (35), (36), it is obvious on making the change of variables of integration, $b = \alpha b'$, $db = \alpha db'$, that the expressions for $M^{(n)}(\Delta\omega_\mu)$, $L^{(n)}(\Delta\omega_\mu)$ are actually independent of α . However, when the transition to the Anderson cut-off procedure is made via eqn (37), where b_0 is to be interpreted as an effective minimum impact parameter, the results are no longer independent of α .

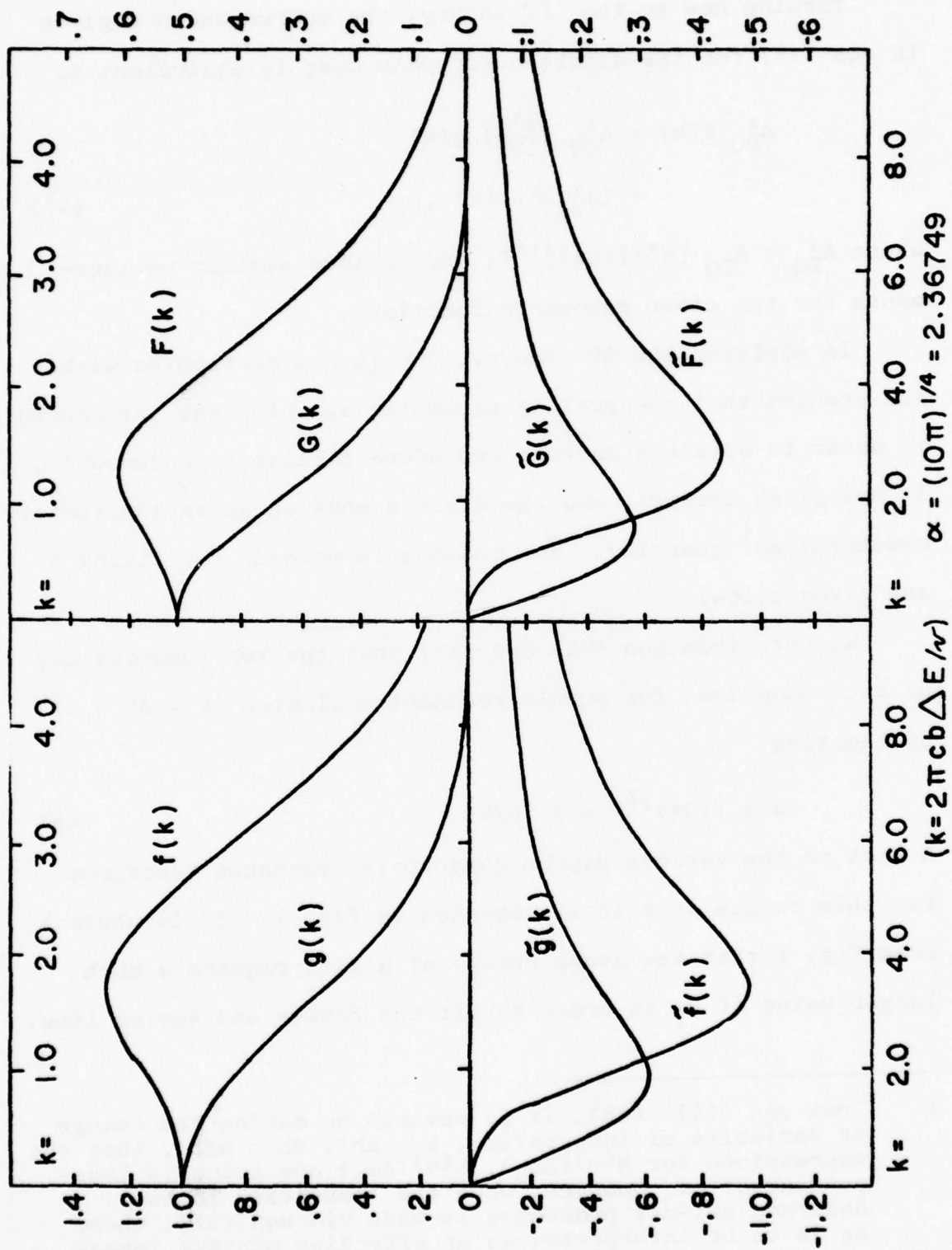


FIGURE 1

Again taking $d_1 = 1.85$ Debye as the H_2O dipole moment, we obtain a fit if $Q_2 = 4.61 \times 10^{-26}$ esu-cm². This value seems far too high, however, we will retain it for purposes of comparison. We shall refer to the results derived from the above choice of parameters as QFT I.

A second method of proceeding is to choose the "best available" value,⁽²³⁾ $Q_2 = 3.04 \times 10^{-26}$ esu-cm², and then to fix α from the calibration line. This yields $\alpha = 2.79$, which is 18% higher than the previous choice. The results derived from this second set of parameters will be denoted by QFT II.

Our final results indicate that the difference between line widths as calculated using the two sets of parameters is never very great. This has the positive implication that the calculated widths are fairly insensitive to the combined choice for (Q_2, α) over a reasonable range, however, it also implies that Q_2 cannot be accurately determined in the present theory. As pointed out in the Introduction, it appears that the overall rms error between theory and experiment at low J (for both the ATC and QFT theories) could be reduced by placing somewhat less weight on the Becker and Autler transition. However, in this paper we are more interested in comparing trends than obtaining a best-fit to the available data. The latter procedure would surely require great selectivity, owing to the difference and accuracy of the experimental procedures used to gather the data.

To complete the discussion of the calculational procedures, we make the following remarks. Since most of the experimental results are confined to the temperature range 295-300°K, we have performed all calculations at 297°K. We have also carried out the calculations for pure N₂, using 30 occupied N₂ levels, and the rotational constant for N₂ was chosen as 2.0 cm⁻¹. It should also be noted that many of the quoted experimental results are for air rather than pure nitrogen. We have not attempted to correct for this, however, from Ref. (14), one expects nitrogen-broadened widths to be approximately 10% higher for low J transitions. For very high J, this is probably no longer true since the scattering cross section is dominated by $\sigma_{HS} = \pi b_{min}^2$. Finally, in the case of the QFT calculations, it may be noted from eqn (41)-(44) that the resonance functions $g(k)$, $G(k)$, $\tilde{g}(k)$, $\tilde{G}(k)$ are functions only of the parameter

$$K = k/\alpha = 2\pi cb\Delta E/\alpha v . \quad (49)$$

This results in a considerable computational simplification because the resonance functions can be tabulated once and for all as a function of K , and then used according to eqn (49). The remaining dependence on α can be lumped into the coupling constant A'_{DQ} as indicated in eqn (47).

The results of our calculations for half-widths are presented in Appendix B where we have divided the transitions into three distinct groups; Group B1 lines with negligible sensitivity to letting $b_{min} < 3.2\overset{\circ}{\text{\AA}}$, Group B2 lines with some

weak sensitivity to the reduction of b_{\min} , and Group B3 lines which are strongly dependent on the choice of b_{\min} .

For the low and intermediate J lines listed in Group B1, we note that the QFT and ATC calculations lead to substantial agreement, the general trend being that the QFT widths are smaller than the ATC widths, with maximum differences of order 5%. We also note that the QFT I results are consistently smaller than the QFT II results, however, the differences are typically of order 1%. Therefore, the distinction between QFT I and QFT II will not be belabored in the discussion which follows. Although the overall comparison of the theoretical and experimental results is not completely satisfactory, we note that most of the large discrepancies are associated with the measurements of Refs. (8), (9), where the observed widths are consistently high compared to the theoretical values. It should be noted that the results in Ref. (9) are for air-broadening, while the calculated widths refer to N_2 -broadening.

The Group B2 lines of intermediate J-values ($8 \leq J \leq 13$) exhibit the same general trends, except that they show some sensitivity to the reduction of b_{\min} below the BK value of 3.20\AA . The QFT results exhibit the greater sensitivity, due to the Gaussian decay of the QFT resonance functions $g(k)$, $G(k)$ at large inelasticities. For these transitions, we note, if b_{\min} is reduced to a value of 1.50\AA , that the theoretical widths are in poor agreement with the observed values of

Ref. (9); however, they are in reasonably good agreement with the measurements of Refs. (15), (16). Of these measurements, only one⁽¹⁵⁾ is a tunable laser observation.

The Group B3 lines, involving high J values, are seen to be extremely sensitive to the choice of b_{\min} . In Fig. 2, we present a plot of half-width vs. b_{\min} for the transition 15, 0, 15 \rightarrow 16, 1, 16. It is seen, if one is willing to allow values of b_{\min} as small as 1.5\AA , that the QFT theory can account for the narrow measured width. The ATC theory, on the other hand, saturates at a value for the half-width of $0.010\text{ cm}^{-1}/\text{atm}$.

It seems clear that no theory such as Anderson's (or the QFT theory as used here), which treats the width as a sum of two independent contributions from a long and short-range part, and which further approximates the short-range part by classical hard-sphere scattering, can provide much further theoretical understanding of the narrow lines at high J. The argument for this is simple. In the present approaches, the scattering cross section may be written

$$\sigma = \sigma_{\text{S.R.}} + \sigma_{\text{L.R.}} = \pi b_{\min}^2 + \sigma_{\text{L.R.}}, \quad (50)$$

where, in the case of interest here, $\sigma_{\text{L.R.}}$ arises from the dipole-quadrupole interaction.

We imagine that it were possible to calculate $\sigma_{\text{L.R.}}$ exactly or to any required high order in perturbation theory. Now $\sigma_{\text{L.R.}}$ is necessarily positive or zero. The best one can hope for is that an exact calculation (for high J transitions)

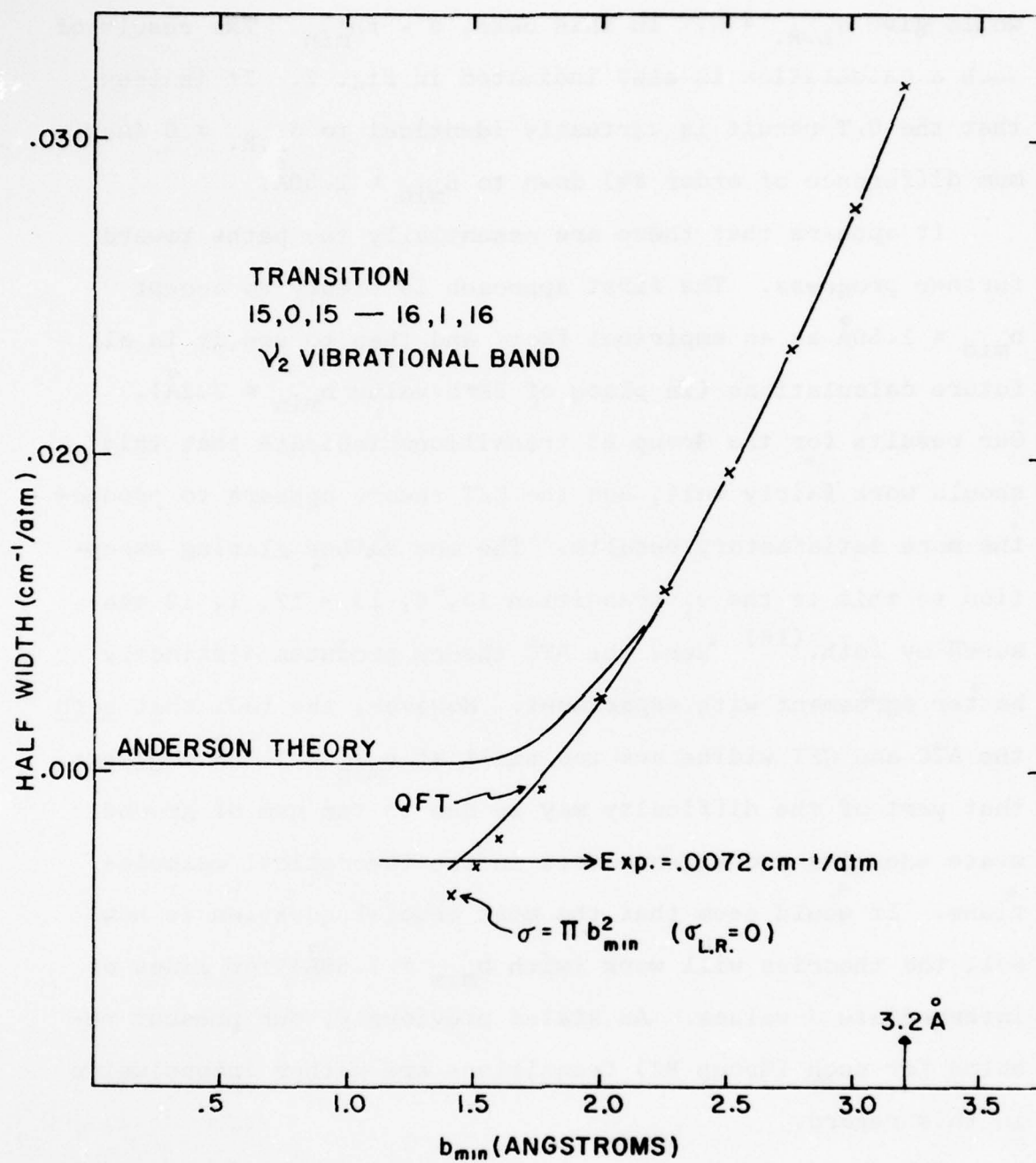


FIGURE 2

would give $\sigma_{L.R.} = 0$. In this case, $\sigma = \pi b_{\min}^2$. The result of such a calculation is also indicated in Fig. 2. It is seen that the QFT result is virtually identical to $\sigma_{L.R.} = 0$ (maximum difference of order 8%) down to $b_{\min} = 1.50\text{\AA}$.

It appears that there are essentially two paths toward further progress. The first approach is simply to accept $b_{\min} = 1.50\text{\AA}$ as an empirical fact, and then to use it in all future calculations (in place of BK's value $b_{\min} = 3.2\text{\AA}$). Our results for the Group B3 transitions indicate that this should work fairly well, and the QFT theory appears to produce the more satisfactory results. The one rather glaring exception to this is the v_1 transition $13, 0, 13 \rightarrow 12, 1, 12$ measured by Toth.⁽¹⁶⁾ Here the ATC theory produces distinctly better agreement with experiment. However, the fact that both the ATC and QFT widths are too small at $b_{\min} = 1.50\text{\AA}$ suggests that part of the difficulty may be due to the use of ground state energies and eigenvectors in the theoretical calculations. It would seem that the most crucial question is how well the theories will work (with $b_{\min} = 1.50\text{\AA}$) for lines of intermediate J values. As stated previously, our present results for such (Group B2) transitions are rather inconclusive in this regard.

The second (obviously more difficult) approach is to try to formulate the detailed interaction which takes place at small intermolecular separations. Such a theory must account, at least qualitatively, for the strong repulsive exchange in-

teractions which occur when the electron clouds overlap, and must yield the dipole-quadrupole interaction at larger separations. Unless a "potential" to describe such effects can be formulated semi-rigorously from first principles, we visualize that the results of such a theory would largely be a reflection of whatever parameters were initially built in to specify the interaction.

A final point to be made in this connection is that the QFT result given in eqn (4), i.e. the probability for a collision involving inelasticity, ΔE , is Gaussian, is very general. In particular, it assumes only conservation of energy and momentum, and a Boltzmann distribution of velocities. It can be applied to any potential (phenomenological or otherwise) for which the Fourier transform exists, and which can be treated using second-order perturbation theory. Although both of these assumptions run into difficulty at very close molecular separations, the implication of weak collisions for high J states seems valid.

The results of our calculations of pressure shifts for measured v_2 transitions are presented in Appendix C. The theoretical calculations (from both theories) show no relation to the experimental results for the two high J lines 15, 1, 15 \rightarrow 16, 0, 16 and 14, 1, 14 \rightarrow 15, 0, 15. No explanation for this difficulty is presently available, although one possible interpretation is that the shift for these high J transitions cannot be correctly calculated without treating the short-range interactions in detail.

For the remaining low J transitions, the QFT theory gives the correct sign of the shift for all six lines, and yields numerically accurate values for four of these transitions. It is also interesting to "interpret" the frequency shift in terms of the individual level shifts of the lower and upper radiative states. Such an interpretation is not completely unambiguous since the determination of b_0 is a joint property of the initial and final states i, f . The results of such an interpretation are shown schematically in Fig. 3 for the three transitions $8, 3, 5 \rightarrow 9, 4, 6$; $6, 4, 2 \rightarrow 7, 5, 3$ and $5, 0, 5 \rightarrow 6, 3, 4$. The results for the other three low J transitions of Appendix C are essentially identical to the situation depicted in Fig. 3b. From Fig. 3, we note the following results: (1) in all cases the signs of the individual level shifts are identical from the ATC and QFT calculations, (2) in most cases the shift of the lower (ground) state level is larger than the upper (v_2) state shift, (3) only in the case of the $5, 0, 5$ state is the level shift negative. Regarding point (2), the ATC result for the transition $8, 3, 5 \rightarrow 9, 4, 6$ is anomalous in that the upper state shift is greater than the lower state shift and this leads to a positive frequency shift.

Concerning the sign of the level shifts, it is easy to see that the contribution to the shift of state i from a collision $i \rightarrow i', J_2 \rightarrow J_2'$ will be positive (negative) when $k_{i0} = (2\pi cb_0/v) (E_i - E_{i'} + E_{J_2} - E_{J_2'})$ is positive (negative). The

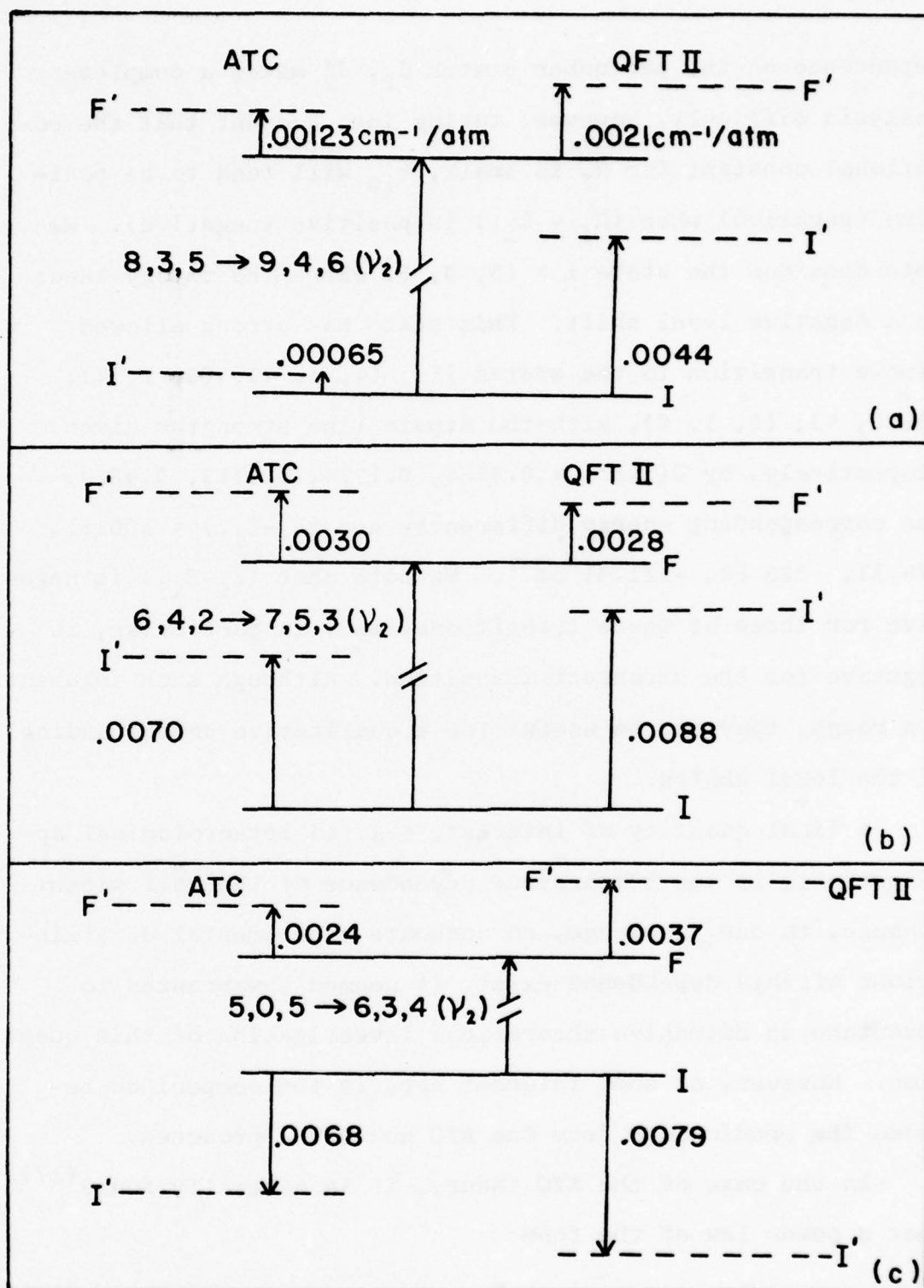


FIGURE 3

dependence on the perturber states J_2, J_2' makes a complete analysis difficult, however, taking into account that the rotational constant for N_2 is small, k_{i0} will tend to be positive (negative) when $(E_i - E_{i'})$ is positive (negative). We then consider the state $i = (5, 0, 5)$ where the theory leads to a negative level shift. This state has strong allowed dipole transition to the states $i' = (4, 1, 4), (5, 1, 4), (6, 3, 4), (6, 1, 6)$, with the dipole line strengths given, respectively, by $D(i, i') = 0.3554, 0.1774, 0.0113, 0.4524$. The corresponding energy differences are $(E_i - E_{i'}) = 100.51, -74.11, -323.64, -121.91 \text{ cm}^{-1}$. We note that $(E_i - E_{i'})$ is negative for three of these transitions, and, in particular, is negative for the strongest transition. Although such arguments are rough, they may be useful for a qualitative understanding of the level shifts.

A final quantity of interest, e.g. to meteorological applications, is the temperature dependence of the half width. Because, to our knowledge, no accurate experimental determinations of this dependence exist, it seemed unwarranted to undertake an extensive theoretical investigation of this question. However, of some interest here is the comparison between the predictions from the ATC and QFT approaches.

In the case of the ATC theory, it is generally found⁽¹⁷⁾ that a power law of the form

$$\gamma(T)/\gamma(T_0) = (T_0/T)^m, \quad (51)$$

adequately describes the temperature dependence. We have

also found this to be true in the QFT theory, at least for low J transitions (where the choice of b_{\min} plays no role). Results for the exponent, m , for four lines of relatively low J are shown below in Table I. We see from the results in Table I that the two theories are fairly consistent, with maximum differences of order 8%. The results at low J are also roughly consistent with an effective cross section which is temperature independent, i.e. the prefactor nv in eqn (5) is proportional to $(T)^{-1/2}$; hence, an average effective cross section which is temperature independent would yield $m = 0.50$.

At high J, e.g. the v_2 transition 15, 0, 15 \rightarrow 16, 1, 16, we find a complicated temperature dependence, which also depends sensitively on the choice of b_{\min} . For example, if we choose $b_{\min} = 1.50 \text{ \AA}$ for the above transition, we find drastic deviations from the power law of eqn (51); the temperature dependence of $\gamma(T)$ is much smaller than at low J, and the Anderson theory leads to a positive temperature dependence [corresponding to m being negative in eqn (51)] while the QFT theory predicts a negative temperature dependence. An experimental investigation of this question would be interesting but probably extremely difficult due to the narrow line width and relatively slow temperature dependence (in going from 225°K to 350°K the ATC and QFT theories predict a change in γ of +16% and -11% respectively).

In conclusion, we offer the following appeal for further experimental studies:

Table I. m eqn (51).

Transition	BK	ATC (Present Results)*	QFT I	QFT II
5,2,3 \rightarrow 6,1,6	0.626	0.629	0.621	0.636
2,2,0 \rightarrow 3,1,3	0.649	0.659	0.664	0.673
6,4,2 \rightarrow 7,5,3 [†]	0.408	0.466	0.425	0.454
1,1,0 \rightarrow 2,2,1	0.616	0.620	0.578	0.602
<p>* Present results derived for $225 < T < 350^\circ\text{K}$; the BK results were derived for $200 < T < 300^\circ\text{K}$.</p>				

[†] ν_2 transition; all others are pure rotational transitions.

(a) It would be valuable to use high resolution tunable lasers to remeasure (in the ν_2 band) some of the low J transitions studied in Refs. (8), (9). The Sanderson and Ginsberg measurement of the $1, 1, 0 \rightarrow 2, 2, 1$ transition remains as a particularly acute embarrassment to the theories. For the low J transitions, we have generally found good agreement between the results from the ATC and QFT calculations, and these are lines for which the long-range dipole-quadrupole interaction is dominant, with very weak dependence on the choice of b_{\min} . Drastic discrepancies between theory and experiment for these lines can only result from the inherent uncertainty associated with the Anderson cut-off method, or possibly with the use of second-order perturbation theory to describe the scattering processes.

(b) In order to ascertain the effect of reducing b_{\min} to a value of 1.50\AA , it would be useful to make a number of high resolution measurements of widths for transitions involving intermediate J values, e.g. J's in the range $9 \lesssim J \lesssim 13$. These lines, theoretically, will exhibit some distinct dependence on whether one chooses $b_{\min} = 3.20\text{\AA}$ (the BK value), or the choice $b_{\min} = 1.50\text{\AA}$ which is suggested from the measurements of Eng at high J.

(c) It would be extremely useful to collect additional laser measurements of H_2O pressure shifts. This is an area where the difference between the ATC and QFT calculations can be pronounced even at low J values. Such measurements could help to differentiate the merits of the two approaches.

If satisfactory resolutions of some of the above uncertainties can be obtained, it would appear that the theory presented here can be applied with rather good confidence to widths of $\text{H}_2\text{O}-\text{N}_2$ over a wide range of J values. The calculation of shifts is more delicate, and the success of the present calculations appears to be limited to low or intermediate J transitions. Additional experimental results should delineate the range of validity.

ACKNOWLEDGEMENTS

We would like to thank S. A. Clough and F. X. Kneizys for numerous helpful discussions, and for the use of their asymmetric rotor computer programs.

REFERENCES

1. V. E. ZUEV, Atmospheric Transparency in the Visible and the Infrared, Keter, Jerusalem (1970).
2. G. E. BECKER and S. H. AUTLER, Phys. Rev. 70, 300 (1946).
3. H. J. LIEBE and T. A. DILLON, J. Chem. Phys. 50, 727 (1969).
4. J. R. RUSK, J. Chem. Phys. 42, 493 (1965).
5. R. EMERY, Infrared Phys. 12, 65 (1972).
6. L. FRENKEL and D. WOODS, Proc. IEEE 54, 498 (1966).
7. J. E. PEARSON, D. T. LLEWELLYN-JONES and R. J. KNIGHT, Infrared Phys. 9, 53 (1969).
8. R. B. SANDERSON and N. GINSBURG, JQSRT 3, 435 (1963).
9. J. R. IZATT, H. SAKAI and W. S. BENEDICT, J. Opt. Soc. Amer. 59, 19 (1969).
10. M. A. GUERRA, M. KETABI, A. SANCHEZ, M. S. FELD and A. JAVAN, J. Chem. Phys. 63, 1317 (1975).
11. F. A. BLUM, K. A. NILL, P. L. KELLEY, A. R. CALAWA and T. C. HARMAN, Science 177, 694 (1972).
12. R. S. ENG, A. R. CALAWA, T. C. HARMAN, P. L. KELLEY and A. JAVAN, Appl. Phys. Lett. 21, 303 (1972).
13. R. S. ENG, P. L. KELLEY, A. MOORADIAN, A. R. CALAWA and T. C. HARMAN, Chem. Phys. Lett. 19, 524 (1973).
14. R. S. ENG, P. L. KELLEY, A. R. CALAWA, T. C. HARMAN and K. W. NILL, Molecular Phys. 28, 653 (1974).
15. C. K. N. PATEL, Phys. Rev. Lett. 28, 649 (1972).
16. R. A. TOTH, JQSRT 13, 1127 (1973).
17. W. S. BENEDICT and L. D. KAPLAN, J. Chem. Phys. 70, 388 (1959).
18. P. W. ANDERSON, Ph.D. Thesis Dissertation, Harvard University (1949).

19. P. W. ANDERSON, Phys. Rev. 76, 647 (1949).
20. C. J. TSAO and B. CURNUTTE, JQSRT 2, 41 (1962).
21. G. BIRNBAUM, Adv. Chem. Phys. 12, 487 (1967).
22. W. S. BENEDICT and L. D. KAPLAN, JQSRT 4, 453 (1964).
23. D. E. STOGRYN and A. P. STOGRYN, Molecular Phys. 11, 371 (1966).
24. J. O. HIRSCHFELDER, C. F. CURTISS and R. B. BIRD, Molecular Theory of Gases and Liquids, Wiley, New York (1964).
25. R. A. McCLATCHEY, W. S. BENEDICT, S. A. CLOUGH, D. E. BURCH, R. A. CALFEE, K. FOX, L. S. ROTHMAN and J. S. GARING, AFCRL Atmospheric Absorption Line Parameters Compilation, AFCRL-TR-73-0096, Environmental Research Papers, No. 434, Air Force Cambridge Research Laboratories, L. G. Hanscom Air Force Base, Bedford, Massachusetts 01731 (26 January 1973).
26. R. W. DAVIES, Phys. Rev. A12, 927 (1975).
27. A. D. BUCKINGHAM, Quart. Rev. (London) 13, 183 (1959).
28. R. M. HERMAN, Phys. Rev. 132, 262 (1963).
29. J. S. MURPHY and J. E. BOGGS, J. Chem. Phys. 54, 2443 (1972).
30. S. C. MEHROTRA and J. E. BOGGS, J. Chem. Phys. 66, 5306 (1977).
31. H. BATEMAN, in Tables of Integral Transforms, edited by A. Erdelyi, McGraw-Hill, New York, Vol. 2, 239 (1954).
32. R. BALESCU, Statistical Mechanics of Charged Particles, 110, Interscience, London (1963).
33. B. D. FRIED and S. D. CONTE, The Plasma Dispersion Function, Academic Press, New York (1961).
34. J. K. G. WATSON, J. Chem. Phys. 46, 1935 (1967); 48, 4517 (1968).
35. S. A. CLOUGH, Y. BEERS, G. P. KLEIN and L. S. ROTHMAN, J. Chem. Phys. 59, 2254 (1973).

36. W. HEITLER, The Quantum Theory of Radiation, Third Edition, p. 69, Oxford University Press, New York and London (1957).
37. D. M. GATES, R. F. CALFEE, D. W. HANSEN and W. S. BENEDICT, "Line Parameters and Computed Spectra for Water Vapor Bands at 2.7μ ," Natl. Bur. Std. Monograph 71, Washington, D. C. (1964).

APPENDIX A

SECOND-ORDER PRESSURE SHIFTS IN THE ANDERSON FORMALISM

Let us begin with the integral equation for the T matrix in Anderson's theory

$$T(t) = 1 - \left(\frac{i}{\hbar}\right) \int_{-\infty}^t \bar{H}_C(t') T(t') dt' , \quad (A1)$$

$$\bar{H}_C(t') = e^{iH_0 t'/\hbar} H_C(t') e^{-iH_0 t'/\hbar} , \quad (A2)$$

where H_0 is the unperturbed Hamiltonian, and $H_C(t')$ is the collision Hamiltonian with the classical-path time-dependence. Iteration of (A1) leads to the series given in eqn (49) of Anderson's original paper.⁽¹⁹⁾ Similarly,

$$T(t)^{-1} = T(t)^\dagger = 1 + \left(\frac{i}{\hbar}\right) \int_{-\infty}^t T(t')^{-1} \bar{H}_C(t') dt' . \quad (A3)$$

Iteration of eqn (A1), (A3) to second order yields

$$T = \lim_{t \rightarrow \infty} T(t) = T_0 + T_1 + T_2 + \dots ,$$

$$T^{-1} = \lim_{t \rightarrow \infty} T(t)^{-1} = T_0^{-1} + T_1^{-1} + T_2^{-1} + \dots , \quad (A4)$$

with

$$T_0 = T_0^{-1} = 1 ,$$

$$T_1 = - T_1^{-1} = - iP , \quad (A5)$$

where (in Anderson's notation)

$$P = \frac{1}{\hbar} \int_{-\infty}^{\infty} H_C(t') dt' , \quad (A6)$$

$$T_2 = -\frac{1}{\hbar^2} \int_{-\infty}^{\infty} dt' \int_{-\infty}^{t'} dt'' \bar{H}_C(t') \bar{H}_C(t'') , \quad (A7)$$

$$T_2^{-1} = -\frac{1}{\hbar^2} \int_{-\infty}^{\infty} dt' \int_{-\infty}^{t'} dt'' \bar{H}_C(t'') \bar{H}_C(t') . \quad (A8)$$

If the non-commutivity of $\bar{H}_C(t')$, $\bar{H}_C(t'')$ in eqn (A7), (A8) is ignored, then by a standard trick of interchanging the names of the dummy variables of integration, one obtains the result of eqn (51) in Anderson's paper, i.e.

$$T_2 = T_2^{-1} = -\frac{1}{2} P^2 . \quad (A9)$$

Now, for the calculation of the cross section, one requires diagonal matrix elements of T_2 . From Anderson's approximation (A9) one then finds

$$\begin{aligned} \langle n | T_2 | n \rangle &= -\frac{1}{2} \langle n | P^2 | n \rangle \\ &= -\frac{1}{2} \sum_{n'} \langle n | P | n' \rangle \langle n' | P | n \rangle \\ &= -\frac{1}{2} \sum_{n'} |\langle n | P | n' \rangle|^2 \\ &= -\frac{1}{2} \sum_{n'} \left| \frac{1}{\hbar} \int_{-\infty}^{\infty} dt e^{i\omega_{nn'}t} \langle n | H_C(t) | n' \rangle \right|^2 , \end{aligned} \quad (A10)$$

where $\omega_{nn'} = \omega_n - \omega_{n'} = (E_n^{(0)} - E_{n'}^{(0)})/\hbar$. If we define the Fourier transform

$$H_C(\omega) = \int_{-\infty}^{\infty} dt e^{i\omega t} H_C(t) , \quad (A11)$$

then eqn (A10) may be written

$$\langle n | T_2 | n \rangle = -\frac{1}{2} \sum_{n'} \left| \frac{1}{\hbar} \langle n | H_C(\omega_{nn'}) | n' \rangle \right|^2 . \quad (A12)$$

The correct treatment of eqn (A7), on the other hand, yields

$$\begin{aligned} \langle n | T_2 | n \rangle = & \sum_{n'} \left(-\frac{1}{\hbar^2} \right) \int_{-\infty}^{\infty} dt' \int_{-\infty}^{t'} e^{i\omega_{nn'}t'} e^{i\omega_{n'n}t''} \\ & \cdot \langle n | H_c(t') | n' \rangle \langle n' | H_c(t'') | n \rangle . \end{aligned} \quad (A13)$$

The trick now is to introduce the inverse Fourier transform

$$H_c(t) = \frac{1}{2\pi} \int_{-\infty}^{\infty} d\omega H_c(\omega) e^{-i\omega t}. \quad (A14)$$

Making use of this in eqn (A13) gives

$$\begin{aligned} \langle n | T_2 | n \rangle = & -\frac{1}{(2\pi\hbar)^2} \sum_{n'} \int_{-\infty}^{\infty} d\omega' \int_{-\infty}^{\infty} \langle n | H_c(\omega') | n' \rangle \langle n' | H_c(\omega'') | n \rangle \\ & \cdot \int_{-\infty}^{\infty} dt' e^{i(\omega_{nn'} - \omega')t'} \int_{-\infty}^{t'} dt'' e^{-i(\omega_{nn'} + \omega'')t''} . \end{aligned} \quad (A15)$$

The integration over t'' yields (36)

$$\begin{aligned} & \int_{-\infty}^{t'} dt'' e^{-i(\omega_{nn'} + \omega'')t''} \\ & = e^{-i(\omega_{nn'} + \omega'')t'} [\pi\delta(\omega_{nn'} + \omega'') + i \frac{\text{Pr}}{\omega_{nn'} + \omega''}] . \end{aligned} \quad (A16)$$

The t' integration then simply gives

$$\int_{-\infty}^{\infty} dt' e^{-i(\omega' + \omega'')t'} = 2\pi\delta(\omega' + \omega'') . \quad (A17)$$

When the integration over ω'' is eliminated, we obtain (with $\omega' \rightarrow \omega$)

$$\begin{aligned} \langle n | T_2 | n \rangle = & -\frac{1}{\hbar^2} \frac{1}{2\pi} \sum_{n'} \int_{-\infty}^{\infty} d\omega \langle n | H_c(\omega) | n' \rangle \langle n' | H_c(-\omega) | n \rangle \\ & \cdot [\pi\delta(\omega_{nn'} - \omega) + i \frac{\text{Pr}}{\omega_{nn'} - \omega}] . \end{aligned} \quad (A18)$$

Since $H_c(t)$ is Hermitian,

$$\langle n' | H_c(-\omega) | n \rangle = \langle n | H_c(\omega) | n' \rangle^* , \quad (A19)$$

so that

$$\begin{aligned} \langle n | T_2 | n \rangle &= -\frac{1}{2} \sum_{n'} \left| \frac{1}{\hbar} \langle n | H_c(\omega_{nn'}) | n' \rangle \right|^2 \\ &+ \frac{i}{2} \sum_{n'} \frac{\text{Pr}}{\pi} \int_{-\infty}^{\infty} \frac{d\omega}{\omega - \omega_{nn'}} \left| \frac{1}{\hbar} \langle n | H_c(\omega) | n' \rangle \right|^2 . \end{aligned} \quad (A20)$$

A little consideration shows that $\langle n | T_2^{-1} | n \rangle = \langle n | T_2 | n \rangle^*$.

We now note that the real part of eqn (A20) is identical to Anderson's result of eqn (A12), and this gives the usual contribution of $S_2(b)_{\text{outer}}$ to the line width. The imaginary term in eqn (A20) yields the second-order shift contribution, and this term is precisely the Hilbert transform of the width function. Subsequent reduction of the cross section using the standard ATC methods then leads directly to eqn (13a) for $s_{\text{if}, J_2}^{(I)}(b)$.

Finally, to obtain

$$S_{\text{if}, J_2}^{(I)}(b_0) = \frac{1}{b_0^2} \int_{b_0}^{\infty} 2b db s_{\text{if}, J_2}^{(I)}(b) , \quad (A21)$$

we require integrals of the form

$$I = \frac{1}{b_0^2} \int_{b_0}^{\infty} \frac{2b db}{b^n} \tilde{f}(k_i) , \quad (A22)$$

where $k_i = b \Delta\omega_i/v$. Since

$$\tilde{f}(k_i) = \frac{\text{Pr}}{\pi} \int_{-\infty}^{\infty} \frac{f(k') dk'}{k' - k_i} ,$$

we need

$$I = \frac{1}{b_0^2} \int_{b_0}^{\infty} \frac{2b db}{b^n} \frac{\text{Pr}}{\pi} \int_{-\infty}^{\infty} \frac{f(k') dk'}{k' - \frac{b \Delta \omega_i}{v}} . \quad (\text{A23})$$

We let $k' = b\omega'/v$ where ω' is the new variable of integration, and then reverse the orders of integration. This gives

$$\begin{aligned} I &= \frac{\text{Pr}}{\pi} \int_{-\infty}^{\infty} \frac{d\omega'}{\omega' - \Delta \omega_i} \frac{2}{b_0^2} \int_{b_0}^{\infty} f(b\omega'/v) \frac{bdb}{b^n} \\ &= \frac{1}{b_0^n} \frac{\text{Pr}}{\pi} \int_{-\infty}^{\infty} \frac{d\omega'}{\omega' - \Delta \omega_i} 2b_0^{n-2} \int_{b_0}^{\infty} \frac{bdb}{b^n} f(b\omega'/v) . \end{aligned} \quad (\text{A24})$$

Next, we let $b = kv/\omega'$ and obtain

$$I = \frac{1}{b_0^n} \frac{\text{Pr}}{\pi} \int_{-\infty}^{\infty} \frac{d\omega'}{\omega' - \Delta \omega_i} 2k_0^{n-2} \int_{k_0}^{\infty} \frac{k dk}{k^n} f(k) , \quad (\text{A25})$$

where $k_0 = b_0 \omega'/v$. From eqn (15a), this is just

$$I = \frac{1}{b_0^n} \frac{\text{Pr}}{\pi} \int_{-\infty}^{\infty} \frac{d\omega'}{\omega' - \Delta \omega_i} F(k_0) . \quad (\text{A26})$$

Finally, multiplying the numerator and denominator of eqn (A26) by b_0/v , yields

$$I = \frac{1}{b_0^n} \frac{\text{Pr}}{\pi} \int_{-\infty}^{\infty} \frac{dk_0 F(k_0)}{k_0 - k_{i0}} = \frac{\tilde{F}(k_{i0})}{b_0^n} , \quad (\text{A27})$$

where $k_{i0} = b_0 \Delta \omega_i / v$. This analysis immediately yields eqn (13b) of Sec. 2.

APPENDIX B

HALF WIDTHS FOR MEASURED N₂ (OR AIR) BROADENED H₂O TRANSITIONS

The following lines show applicable values for the succeeding table. Common parameters: $T = 297^\circ\text{K}$, $d_1 = 1.85 \times 10^{-18}$ esu-cm (ground state), $d_1 = 1.82 \times 10^{-18}$ esu-cm (v_2 state). Anderson Theory: $Q_2 = 3.00 \times 10^{-26}$ esu-cm². QFT I: $Q_2 = 4.61 \times 10^{-26}$ esu-cm², $\alpha = (10\pi)^{1/4} = 2.36749$. QFT II: $Q_2 = 3.04 \times 10^{-26}$ esu-cm², $\alpha = 2.79$. Half widths in cm⁻¹/atm. () = Results of Benedict and Kaplan at 300°K; for Ref. (16), theoretical values as quoted from Gates, et. al; ⁽³⁷⁾ rot = pure rotational transition.

GROUP B1

Lower \rightarrow Upper (J, K_a, K_c)

Transition	ATC	QFT I	QFT II	Experiment & Reference
5,2,3 \rightarrow 6,1,6 rot.	0.10046 (0.090)	0.10045	0.10050	(calibration line) 0.087 (Air, 318°K), Ref. (2) 0.104 (N ₂ , 300°K), Ref. (3)
2,2,0 \rightarrow 3,1,3 rot.	0.10683 (0.096)	0.10610	0.10629	0.095 (N ₂), Ref. (4) 0.111 (N ₂ ²), Ref. (5) 0.111 (N ₂ ²), Ref. (6)
3,2,1 \rightarrow 4,1,4 rot.	0.10558 (0.095)	0.10379	0.10443	0.095 (Air), Ref. (7)
1,1,0 \rightarrow 2,2,1 rot.	0.11354 (0.102)	0.10644	0.10845	0.18 (N ₂), Ref. (8)
3,2,1 \rightarrow 4,3,2 rot.	0.09662 (0.087)	0.09555	0.09591	0.12 (N ₂), Ref. (8)
4,2,2 \rightarrow 5,3,3 rot.	0.09919 (0.089)	0.09792	0.09836	0.13 (N ₂), Ref. (8)
5,3,3 \rightarrow 6,6,0 rot.	0.07348 (0.066)	0.07063	0.07148	0.08 (Air), Ref. (9)
5,3,2 \rightarrow 6,6,1 rot.	0.08084 (0.073)	0.07905	0.07984	0.09 (Air), Ref. (9)
6,3,4 \rightarrow 7,6,1 rot.	0.07225 (0.065)	0.06982	0.07043	0.07 (Air), Ref. (9)
6,3,3 \rightarrow 7,6,2 rot.	0.08551 (0.077)	0.08378	0.08464	0.07 (Air), Ref. (9)
6,2,5 \rightarrow 7,5,2 rot.	0.07382 (0.067)	0.07050	0.07132	0.08 (Air), Ref. (9)
6,1,6 \rightarrow 7,4,3 rot.	0.08374 (0.076)	0.08052	0.08137	0.10 (Air), Ref. (9)
7,3,5 \rightarrow 8,6,2 rot.	0.06973 (0.063)	0.06721	0.06772	0.07 (Air), Ref. (9)

GROUP B1 (Continued)

Transition	ATC	QFT I	QFT II	Experiment & Reference
7,3,4 \rightarrow 8,6,3 rot.	0.08920 (0.080)	0.08811	0.08865	0.09 (Air), Ref. (9)
7,2,6 \rightarrow 8,5,3 rot.	0.06865 (0.062)	0.06408	0.06551	0.07 (Air), Ref. (9)
7,1,7 \rightarrow 8,4,4 rot.	0.08412 (0.076)	0.07951	0.08119	0.08 (Air), Ref. (9)
8,2,6 \rightarrow 9,5,5 rot.	0.08356 (0.075)	0.07970	0.08081	0.08 (Air), Ref. (9)
5,1,5 \rightarrow 6,2,4 v_2	0.10178 (0.093)	0.09963	0.10023	0.095 (N_2), Ref. (10)
5,3,2 \rightarrow 6,4,3 v_2	0.08669 (0.080)	0.08498	0.08576	0.103 (N_2), Ref. (10)
8,3,5 \rightarrow 9,4,6 v_2	0.09206 (0.084)	0.08999	0.09074	0.081 (N_2), Refs. (13), (14) 0.073 (Air), Ref. (14)
9,3,6 \rightarrow 10,4,7 v_2	0.08747	0.08157	0.08362	0.089 (N_2), Ref. (14) 0.081 (Air), Ref. (14)
6,1,6 \rightarrow 7,2,5 v_2	0.09293 (0.086)	0.08837	0.08994	0.092 (N_2), Refs. (13), (14) 0.085 (Air), Ref. (14)
6,4,2 \rightarrow 7,5,3 v_2	0.07155 (0.066)	0.06912	0.06986	0.053 (Air), Refs. (13), (14)
6,4,3 \rightarrow 7,5,2 v_2	0.06757 (0.060)	0.06483	0.06558	0.053 (Air), Refs. (13), (14)
5,4,1 \rightarrow 6,5,2 v_2	0.06542 (0.060)	0.06272	0.06350	0.063 (Air), Ref. (13)
5,4,2 \rightarrow 6,5,1 v_2	0.06391 (0.059)	0.06154	0.06214	0.058 (Air), Ref. (13)
5,0,5 \rightarrow 6,3,4 v_2	0.08628 (0.080)	0.08048	0.08233	0.098 (N_2), Ref. (14) 0.088 (Air), Ref. (14)
3,1,2 \rightarrow 4,4,1 v_2	0.09264 (0.085)	0.08698	0.08873	0.096 (N_2), Ref. (14)

GROUP B1 (Continued)

Transition	ATC	QFT I	QFT II	Experiment & Reference
4,2,3 \rightarrow 4,1,4 $2v_2$	0.09941 (0.091)	0.09466	0.09605	0.096 (Air), Ref. (16)
3,2,2 \rightarrow 3,1,3 $2v_2$	0.10401 (0.094)	0.10057	0.10194	0.083 (Air), Ref. (16)
2,1,2 \rightarrow 1,0,1 $2v_2$	0.11723 (0.104)	0.10965	0.11186	0.101 (Air), Ref. (16)
3,0,3 \rightarrow 2,1,2 $2v_2$	0.11051 (0.099)	0.10763	0.10854	0.101 (Air), Ref. (16)
2,2,1 \rightarrow 2,1,2 $2v_2$	0.10597 (0.096)	0.10288	0.10387	0.099 (Air), Ref. (16)
3,3,0 \rightarrow 3,2,1 $2v_2$	0.09499 (0.084)	0.09317	0.09363	0.097 (Air), Ref. (16)
1,1,1 \rightarrow 0,0,0 $2v_2$	0.11084 (0.100)	0.10263	0.10529	0.104 (Air), Ref. (16)
1,1,0 \rightarrow 1,0,1 $2v_2$	0.12340 (0.108)	0.11298	0.11596	0.109 (Air), Ref. (16)
3,1,2 \rightarrow 2,2,1 $2v_2$	0.10559 (0.095)	0.10311	0.10370	0.095 (Air), Ref. (16)
1,0,1 \rightarrow 1,1,0 $2v_2$	0.12340 (0.111)	0.11298	0.11596	0.110 (Air), Ref. (16)
0,0,0 \rightarrow 1,1,1 $2v_2$	0.11084 (0.100)	0.10263	0.10529	0.107 (Air), Ref. (16)
3,0,3 \rightarrow 3,1,2 $2v_2$	0.11031 (0.099)	0.10670	0.10773	0.105 (Air), Ref. (16)
2,2,1 \rightarrow 3,1,2 $2v_2$	0.10559 (0.095)	0.10311	0.10370	0.102 (Air), Ref. (16)
2,1,2 \rightarrow 3,0,3 $2v_2$	0.11051 (0.099)	0.10763	0.10854	0.104 (Air), Ref. (16)
4,0,4 \rightarrow 4,1,3 $2v_2$	0.10830 (0.097)	0.10568	0.10648	0.108 (Air), Ref. (16)

GROUP B1 (Continued)

Transition	ATC	QFT I	QFT II	Experiment & Reference
3,1,2 \rightarrow 3,2,1 $2\nu_2$	0.10498 (0.095)	0.09989	0.10125	0.098 (Air), Ref. (16)
2,1,1 \rightarrow 2,2,0 $2\nu_2$	0.10823 (0.098)	0.10344	0.10463	0.097 (Air), Ref. (16)
5,1,4 \rightarrow 5,2,3 $2\nu_2$	0.10523 (0.095)	0.10284	0.10348	0.105 (Air), Ref. (16)
2,0,2 \rightarrow 3,1,3 $2\nu_2$	0.11379 (0.103)	0.10869	0.11016	0.101 (Air), Ref. (16)
3,1,3 \rightarrow 4,0,4 $2\nu_2$	0.10675 (0.096)	0.10268	0.10401	0.092 (Air), Ref. (16)
2,1,2 \rightarrow 2,2,1 $2\nu_2$	0.10597 (0.095)	0.10288	0.10387	0.105 (Air), Ref. (16)
5,0,5 \rightarrow 5,1,4 $2\nu_2$	0.10153 (0.091)	0.09908	0.09981	0.097 (Air), Ref. (16)
6,1,5 \rightarrow 6,2,4 $2\nu_2$	0.10238 (0.092)	0.09998	0.10072	0.094 (Air), Ref. (16)
3,0,3 \rightarrow 4,1,4 $2\nu_2$	0.10854 (0.098)	0.10590	0.10668	0.099 (Air), Ref. (16)
8,6,3 \rightarrow 7,4,4 ν_3	0.06601 (0.060)	0.06278	0.06365	0.067 (Air), Ref. (16)
4,1,4 \rightarrow 5,0,5 $2\nu_2$	0.09730 (0.088)	0.09076	0.09283	0.089 (Air), Ref. (16)
4,1,4 \rightarrow 4,2,3 $2\nu_2$	0.09941 (0.090)	0.09466	0.09605	0.095 (Air), Ref. (16)
4,0,4 \rightarrow 5,1,5 $2\nu_2$	0.09996 (0.090)	0.09627	0.09734	0.085 (Air), Ref. (16)
7,1,6 \rightarrow 7,2,5 $2\nu_2$	0.09479 (0.085)	0.09043	0.09191	0.082 (Air), Ref. (16)
4,2,3 \rightarrow 5,1,4 $2\nu_2$	0.10215 (0.092)	0.10003	0.10062	0.089 (Air), Ref. (16)

GROUP B1 (Continued)

Transition	ATC	QFT I	QFT II	Experiment & Reference
7,2,5 \rightarrow 7,3,4 $2\nu_2$	0.10288 (0.093)	0.10007	0.10091	0.088 (Air), Ref. (16)
6,2,4 \rightarrow 6,3,3 $2\nu_2$	0.10282 (0.093)	0.09954	0.10070	0.086 (Air), Ref. (16)
7,6,1 \rightarrow 6,4,2 ν_3	0.06341 (0.059)	0.06649	0.06739	0.069 (Air), Ref. (16)
1,1,1 \rightarrow 2,2,0 $2\nu_2$	0.10706 (0.095)	0.10260	0.10407	0.101 (Air), Ref. (16)
9,4,5 \rightarrow 8,3,6 ν_1	0.08830 (0.077)	0.08409	0.08565	0.080 (Air), Ref. (16)
3,2,1 \rightarrow 3,3,0 $2\nu_2$	0.09499 (0.085)	0.09317	0.09363	0.091 (Air), Ref. (16)
4,2,3 \rightarrow 4,3,2 $2\nu_2$	0.09208 (0.083)	0.08882	0.08985	0.084 (Air), Ref. (16)
7,6,1 \rightarrow 6,5,2 ν_1	0.05273 (0.050)	0.04953	0.05041	0.051 (Air), Ref. (16)
6,2,5 \rightarrow 6,3,4 $2\nu_2$	0.08302 (0.075)	0.07957	0.08052	0.071 (Air), Ref. (16)
8,5,4 \rightarrow 7,4,3 ν_1	0.07830 (0.069)	0.07595	0.07668	0.073 (Air), Ref. (16)
4,1,3 \rightarrow 5,2,1 $2\nu_2$	0.10311 (0.093)	0.10123	0.10177	0.090 (Air), Ref. (16)
8,4,5 \rightarrow 7,2,6 ν_3	0.07150 (0.069)	0.06758	0.06867	0.081 (Air), Ref. (16)
7,5,2 \rightarrow 6,4,3 ν_1	0.06931 (0.064)	0.06538	0.06638	0.069 (Air), Ref. (16)
7,5,3 \rightarrow 6,4,2 ν_1	0.07320 (0.066)	0.07001	0.07095	0.072 (Air), Ref. (16)
7,3,4 \rightarrow 7,4,3 $2\nu_2$	0.09746 (0.088)	0.09636	0.09675	0.083 (Air), Ref. (16)

GROUP B1 (Continued)

Transition	ATC	QFT I	QFT II	Experiment & Reference
6,1,5 \rightarrow 7,2,6 $2v_2$	0.08676 (0.078)	0.08439	0.08506	0.089 (Air), Ref. (16)
7,3,4 \rightarrow 6,2,5 v_1	0.09787 (0.084)	0.09645	0.09718	0.082 (Air), Ref. (16)
6,5,1 \rightarrow 5,3,2 v_3	0.08407 (0.070)	0.08172	0.08274	0.076 (Air), Ref. (16)
5,3,2 \rightarrow 5,4,1 $2v_2$	0.08768 (0.079)	0.08635	0.08688	0.084 (Air), Ref. (16)
7,4,3 \rightarrow 6,3,4 v_1	0.08578 (0.078)	0.08268	0.08363	0.077 (Air), Ref. (16)
8,4,5 \rightarrow 7,3,4 v_1	0.09431 (0.080)	0.09338	0.09407	0.090 (Air), Ref. (16)
2,2,1 \rightarrow 3,3,0 $2v_2$	0.09352 (0.084)	0.09136	0.09201	0.083 (Air), Ref. (16)
6,4,3 \rightarrow 6,3,4 $2v_2$	0.07944 (0.072)	0.07530	0.07650	0.071 (Air), Ref. (16)
6,2,4 \rightarrow 5,1,5 v_1	0.10341 (0.087)	0.10215	0.10256	0.097 (Air), Ref. (16)
7,4,4 \rightarrow 6,3,3 v_1	0.09280 (0.079)	0.09113	0.09197	0.086 (Air), Ref. (16)
5,5,0 \rightarrow 4,3,1 v_3	0.07724 (0.065)	0.07506	0.07594	0.077 (Air), Ref. (16)
6,4,3 \rightarrow 5,3,2 v_1	0.08912 (0.077)	0.08791	0.08845	0.083 (Air), Ref. (16)
7,2,5 \rightarrow 6,0,6 v_3	0.09552 (0.079)	0.09165	0.09312	0.084 (Air), Ref. (16)

GROUP B2

Transition	ATC	QFT I	QFT II	Experiment & Reference
9,1,9 → 10,2,8 ₀ rot. b _{min} = 3.20Å 2.50 1.50	(0.054) 0.05816 0.05684 0.05684	0.05371 0.04978 0.04914	0.05493 0.05196 0.05173	0.07 (Air), Ref. (9)
9,2,7 → 10,5,6 ₀ rot. b _{min} = 3.20Å 2.50 1.50	(0.067) 0.07350 0.07335 0.07335	0.06902 0.06749 0.06742	0.07027 0.06939 0.06939	0.10 (Air), Ref. (9)
9,1,8 → 10,4,7 ₀ rot. b _{min} = 3.20Å 2.50 1.50	(0.053) 0.05611 0.05453 0.05453	0.05115 0.04683 0.04613	0.05237 0.04896 0.04870	0.10 (Air), Ref. (9)
10,1,10 → 11,2,9 rot. b _{min} = 3.20Å 2.50 1.50	(0.044) 0.04661 0.04291 0.04273	0.04304 0.03623 0.03410	0.04395 0.03817 0.03700	0.08 (Air), Ref. (9)
10,1,9 → 11,4,8 rot. b _{min} = 3.20Å 2.50 1.50	(0.046) 0.04863 0.04557 0.04550	0.04442 0.03827 0.03669	0.04545 0.04024 0.03944	0.05 (Air), Ref. (9)
10,2,8 → 11,5,7 rot. b _{min} = 3.20Å 2.50 1.50	(0.057) 0.06155 0.06048 0.06048	0.05633 0.05258 0.05203	0.05772 0.05499 0.05483	0.08 (Air), Ref. (9)
10,2,9 → 11,3,8 rot. b _{min} = 3.20Å 2.50 1.50	(0.064) 0.07062 0.07061 0.07061	0.06552 0.06481 0.06481	0.06701 0.06658 0.06658	0.07 (Air), Ref. (9)
11,1,10 → 12,4,9 rot. b _{min} = 3.20Å 2.50 1.50	(0.041) 0.04331 0.03885 0.03856	0.04015 0.03279 0.03037	0.04090 0.03435 0.03290	0.07 (Air), Ref. (9)
11,2,9 → 12,5,8 rot. b _{min} = 3.20Å 2.50 1.50	(0.049) 0.05083 0.04790 0.04784	0.04577 0.03937 0.03759	0.04713 0.04188 0.04103	0.07 (Air), Ref. (9)

GROUP B2 (Continued)

Transition	ATC	QFT I	QFT II	Experiment & Reference
12,3,10 \rightarrow 13,4,9 rot. $b_{\min} = 3.20\text{\AA}$ 2.50 1.50	(0.063) 0.06928 0.06913 0.06913	0.06288 0.06197 0.06197	0.06488 0.06423 0.06423	0.05 (Air), Ref. (9)
10,2,8 \rightarrow 11,3,9 v_2 $b_{\min} = 3.20\text{\AA}$ 2.50 1.50	(0.054) 0.05991 0.05952 0.05952	0.05668 0.05520 0.05518	0.05749 0.05635 0.05635	0.0435 (Air), Ref. (15)
11,1,10 \rightarrow 10,2,9 v_1 $b_{\min} = 3.20\text{\AA}$ 2.50 1.50	(0.044) 0.03320 0.03423 0.03422	0.03721 0.03030 0.02990	0.03769 0.03131 0.03110	0.035 (Air), Ref. (16)
8,7,1 \rightarrow 7,6,2 v_1 $b_{\min} = 3.20\text{\AA}$ 2.50 1.50	(0.042) 0.04430 0.04378 0.04378	0.04153 0.03982 0.03982	0.04219 0.04109 0.04109	0.037 (Air), Ref. (16)
6,1,6 \rightarrow 7,0,7 $2v_2$ $b_{\min} = 3.20\text{\AA}$ 2.50 1.50	(0.063) 0.06836 0.06786 0.06786	0.06127 0.05912 0.05912	0.06325 0.06181 0.06181	0.059 (Air), Ref. (16)
9,0,9 \rightarrow 8,1,8 $2v_2$ $b_{\min} = 3.20\text{\AA}$ 2.50 1.50	(0.044) 0.04567 0.04151 0.04157	0.04107 0.03344 0.03183	0.04229 0.03575 0.03474	0.038 (Air), Ref. (16)
8,2,7 \rightarrow 9,1,8 $2v_2$ $b_{\min} = 3.20\text{\AA}$ 2.50 1.50	(0.05) 0.05433 0.05373 0.05373	0.04943 0.04762 0.04762	0.05088 0.04957 0.04957	0.045 (Air), Ref. (16)

GROUP B3

Transition	A °C	QFT I	QFT II	Experiment & Reference
15,0,15 → 16,1,16 v_2 $b_{\min} = 3.20\text{\AA}$	0.03180	0.03178	0.03179	0.0072 (N ₂), Refs. (12), (13), (14)
2.50	0.01954	0.01941	0.01943	0.0070 (Air), Ref. (14)
2.00	0.01307	0.01248	0.01256	0.0075 (Air), Ref. (11)
1.75	0.01104	0.00965	0.00985	
1.60	0.01043	0.00819	0.00854	
1.50	0.01029	0.00735	0.00785	
1.40	0.01028	0.00663	0.00734	
15,1,15 → 16,0,16 v_2 $b_{\min} = 3.20\text{\AA}$	0.03181	0.03179	0.03179	Exp. results same as above
2.50	0.01954	0.01942	0.01944	
2.00	0.01310	0.01249	0.01253	
1.75	0.01107	0.00967	0.00983	
1.60	0.01047	0.00823	0.00853	
1.50	0.01034	0.00739	0.00790	
1.40	0.01032	0.00668	0.00740	
14,1,14 → 15,0,15 v_2 $b_{\min} = 3.20\text{\AA}$	0.03187	0.03180	0.03182	0.011 (Air), Ref. (13)
2.50	0.01977	0.01947	0.01952	
2.00	0.01378	0.01263	0.01282	
1.75	0.01221	0.00992	0.01032	
1.60	0.01187	0.00859	0.00920	
1.50	0.01184	0.00785	0.00867	
1.40	0.01184	0.00726	0.00833	
14,0,14 → 15,1,15 v_2 $b_{\min} = 3.20\text{\AA}$	0.03186	0.03180	0.03181	Exp. results same as above
2.50	0.01975	0.01946	0.01951	
2.00	0.01374	0.01260	0.01278	
1.75	0.01215	0.00986	0.01025	
1.60	0.01181	0.00850	0.00912	
1.50	0.01178	0.00775	0.00858	
1.40	0.01178	0.00714	0.00823	
12,2,11 → 13,1,12 v_2 $b_{\min} = 3.20\text{\AA}$	0.03341	0.03278	0.03292	0.0185 (N ₂), Ref. (14)
2.50	0.02394	0.02203	0.02249	0.0171 (Air), Refs. (13), (14)
2.00	0.02220	0.01901	0.01990	0.0155 (Air), Ref. (11)
1.75	0.02220	0.01900	0.01990	
1.60	0.02220	0.01900	0.01990	
1.50	0.02220	0.01900	0.01990	
1.40	0.02220	0.01900	0.01990	

GROUP B3 (Continued)

Transition	ATC	QFT I	QFT II	Experiment & Reference
12,1,11 → 13,2,12 v_2 $b_{\min} = 3.20\text{\AA}$	0.03334	0.03278	0.03290	0.0145 (Air), Ref. (11) 0.0170 (Air), Ref. (13)
2.50	0.02344	0.02181	0.02219	
2.00	0.02076	0.01768	0.01835	
1.75	0.02068	0.01699	0.01779	
1.60	0.02068	0.01687	0.01779	
1.50	0.02068	0.01686	0.01779	
1.40	0.02068	0.01686	0.01779	
15,2,14 → 16,1,15 v_2 $b_{\min} = 3.20\text{\AA}$	0.03194	0.03190	0.03191	0.0096 (N ₂), Ref. (14) 0.0091 (Air), Ref. (14) 0.0110 (Air), Ref. (13)
2.50	0.02000	0.01980	0.01984	
2.00	0.01437	0.01365	0.01377	
1.75	0.01316	0.01184	0.01208	
1.60	0.01299	0.01122	0.01152	
1.50	0.01299	0.01098	0.01136	
1.40	0.01299	0.01086	0.01131	
15,1,14 → 16,2,15 v_2 $b_{\min} = 3.20\text{\AA}$	0.03186	0.03182	0.03182	Exp. results same as above
2.50	0.01974	0.01952	0.01956	
2.00	0.01362	0.01279	0.01294	
1.75	0.01185	0.01019	0.01049	
1.60	0.01136	0.00895	0.00941	
1.50	0.01126	0.00828	0.00889	
1.40	0.01125	0.00775	0.00854	
13,0,13 → 12,1,12 v_1 $b_{\min} = 3.20\text{\AA}$	0.03247	0.03207	0.03216	0.0183 (Air), Ref. (16)
2.50	0.02133	0.02003	0.02031	
2.00	0.01701	0.01375	0.01444	
1.75	0.01644	0.01156	0.01268	
1.60	0.01643	0.01064	0.01210	
1.50	0.01643	0.01023	0.01192	
1.40	0.01643	0.00997	0.01187	

APPENDIX C

LINE SHIFTS FOR MEASURED N₂ (OR AIR) BROADENED H₂O TRANSITIONS

Line Shifts in cm⁻¹/atm

Transition	ATC	QFT I	QFT II	Experiment & Reference
Lower → Upper (J, K, K _C) 15, 1, 15 → 16, 0, 16 b _{min} = 3.20 Å 2.50 1.50	0.00035 0.00147 0.00991	0.00039 0.00131 0.01298	0.00038 0.00123 0.01451	-0.0038 (N ₂), Refs. (12), (13) -0.0033 (Air), Ref. (12)
14, 1, 14 → 15, 0, 15 b _{min} = 3.20 Å 2.50 1.50	0.00037 0.00126 0.00865	0.00042 0.00140 0.01783	0.00040 0.00132 0.01563	-0.0041 (Air), Ref. (13)
8, 3, 5 → 9, 4, 6 b _{min} = 3.20 Å 2.50 1.50	0.00058 0.00058 0.00058	-0.00412 -0.00429 -0.00429	-0.00236 -0.00235 -0.00235	-0.0066 (N ₂), Ref. (13)
6, 4, 2 → 7, 5, 3 b _{min} = 3.20 Å 2.50 1.50	-0.00401 -0.00401 -0.00401	-0.00648 -0.00655 -0.00655	-0.00603 -0.00604 -0.00604	-0.0060 (Air), Ref. (13)
6, 4, 3 → 7, 5, 2 b _{min} = 3.20 Å 2.50 1.50	-0.00388 -0.00388 -0.00388	-0.00687 -0.00687 -0.00687	-0.00617 -0.00617 -0.00617	-0.0059 (Air), Ref. (13)
5, 4, 1 → 6, 5, 2 b _{min} = 3.20 Å 2.50 1.50	-0.00421 -0.00421 -0.00421	-0.00733 -0.00755 -0.00755	-0.00648 -0.00657 -0.00657	-0.0070 (Air), Ref. (13)

Transition	ATC	QFT I	QFT II	Experiment & Reference
5,4,2 \rightarrow 5,3,1 $\frac{V}{2}$ $b_{\min} = 3.20\text{\AA}^2$ 2.50 1.50	-0.00433 -0.00433 -0.00433	-0.00722 -0.00752 -0.00752	-0.00648 -0.00666 -0.00666	-0.0070 (Air), Ref. (13)
5,0,5 \rightarrow 6,3,4 $\frac{V}{2}$ $b_{\min} = 3.20\text{\AA}^2$ 2.50 1.50	0.00916 0.00916 0.00916	0.01346 0.01346 0.01346	0.01155 0.01155 0.01155	+0.0044 (Air), Ref. (14)